Ph.D. DISSERTATION

Development of an Implantable Electrical Stimulation Device for Bone Regeneration

골 재생을 위한 이식가능형 전기자극장치의 개발

BY

JUNGHOON KIM

AUGUST 2014

DEPARTMENT OF ELECTRICAL
ENGINEERING AND COMPUTER SCIENCE
COLLEGE OF ENGINEERING
SEOUL NATIONAL UNIVERSITY

Development of an Implantable Electrical Stimulation Device for Bone Regeneration

지도 교수 김 성 준

이 논문을 공학박사 학위논문으로 제출함
2014 년 8 월

서울대학교 대학원
전기컴퓨터공학부
김 정 훈

김정훈의 공학박사 학위논문을 인준함
2014 년 8 월

위 원 장 _____ (인)

부위원장 _____ (인)

위 원 _____ (인)

위 원 _____ (인)

위 원 _____ (인)

Abstract

Electrical stimulation modulates cellular process in a form of ionic current through regulating cell membrane potential. Electrical stimulation has effects of up-regulation of cell proliferation rate and cell viability. As a good osteoinductive tool, electrical stimulation has effects of differentiation to bone cell, acceleration of ossification and calcium induction that improve bone regeneration. Although implantable electrical stimulation devices for bone regeneration were commercialized, there was limitation for applying to bone graft transplantation due to the shape of the device and stimulation delivery.

In the present dissertation, implantable bone regeneration device using electrical stimulation is demonstrated. The device can deliver a concentrated electrical stimulation to three-dimensional bone graft. The evaluation of bone regeneration targeting animal bone defect model using the designed device is demonstrated.

As a preliminary step for developing bone regeneration device, a bioreactor device which allows intracorporeal cell culture using electrical stimulation was designed. Using this device, human mesenchymal stromal cell was cultured intracorporeally with electrical stimulation. The cell proliferation of the electrical stimulated stem cell was increased by 23% compared to the unstimulated stem cell. Also in the electrically stimulated group, stem cell had more stable adhesion to the collagen sponge and better extracellular matrix formation compare to the control group.

Through improvement of the bioreactor device, bone regeneration experiment targeting a rabbit mandible was executed by transplantation of stem cell graft and electrical stimulation device into the defect site. Polyimide electrode was designed to be suited the defect of animal and electrical current generator was packaged with silicone. The electrical stimulated group showed a higher bone volume by 260% compared with unstimulated group. Also electrical stimulated group showed better new bone formation results in various bone parameters.

Then LCP-based bone regeneration device was designed with a built-in electrical current generator and wireless power receiver device. LCP has good hermeticity and good osseo-integration property. This device performs a graft containment system and electrical stimulation device simultaneously.

From these results, bone regeneration treatment using implantable bone regeneration device which can apply electrical stimulation to defect site directly can be an effective and new methods for bone defect recovery. Furthermore, it can be expected that development of implantable bone regeneration device using LCP and development of combined treatment of intracorporeal stem cell culture and electrical stimulation.

Keywords: Electrical stimulation, implantable device, bone regeneration, stem cell, LCP
Student Number: 2009-30184

Contents

Abstract i

Contents iii

List of Figures v

List of Tables vii

Chapter 1 Introduction 1
1.1 Regulation of cellular process through electrical stimulation 1
1.1.1 Charge transfer at interface of electrode/electrolyte 3
1.1.2 Electrical equivalent circuit modeling of cellular membrane 7
1.1.3 Gating mechanisms of ion channels 19
1.1.3.1 Voltage-gated ion channel 21
1.1.3.2 Ligand-gated ion channel 21
1.1.3.3 Second messenger gated ion channel 23
1.1.3.4 Mechanosensitive ion channel 24
1.1.3.5 Light sensitive ion channel 27
1.1.3.6 Temperature sensitive ion channel 29
1.1.4 Cellular processes generated by change of transmembrane potential 32
1.1.4.1 Generation of action potential 32
1.1.4.2 Intracellular second messenger signaling pathway 36
1.2 Bone regeneration using electrical stimulation 38
1.2.1 Bone regeneration process by electrical stimulation 38
1.2.2 Clinical studies of bone regeneration using direct current stimulation 40
1.2.3 Development progress of direct current stimulator for bone regeneration 42
1.3 Bone regeneration therapy 47
1.3.1 Existing bone regeneration therapies 47
1.3.2 Bone regeneration therapy using stem cell graft 49
1.4 LCP as bone substitute 50
1.5 Objectives of the dissertation 52

Chapter 2 Materials and Methods 54
2.1 Implantable bioreactor device 54
2.1.1 Device configuration 54
2.1.2 Bioreactor using titanium electrode 60
2.1.3 Bioreactor using polyimide electrode 62
2.1.4 *In vivo* cell proliferation experiment 65
2.1.4.1 Preparation of collagen sponge 65
2.1.4.2 Preparation of hMSCs 66
2.1.4.3 Process of animal experiment 67
2.1.5 Assessment of cell proliferation 69
2.1.5.1 MTT assay 69
2.1.5.2 Scanning electron microscopy (SEM) 69
2.1.5.3 Reverse transcription=polymerase chain reaction (RT−PCR) 70
2.2 Implantable electrical stimulation device for bone regeneration 71
2.2.1 Configuration of bone regeneration device 71
2.2.2 Electrode for bone regeneration of rabbit mandible 72
2.2.3 Preperation of collagen sponge 73
2.2.4 hBMSCs culture 73
2.2.5 Preperation of hydrogel 74
2.2.6 Preperation of PCL containment system 75
2.2.7 Animal experiment 76
2.2.7.1 Animal experiment configuration 76
2.2.7.2 Animal experiment process 77
2.2.8 Assessment of bone regeneration 79
2.2.8.1 Soft x−ray 79
2.2.8.2 micro CT 80
2.2.8.3 Histochemical staining 81
2.3 LCP based implantable bone regeneration device 82
2.3.1 Device configuration 82
2.3.2 LCP layers for bone regeneration device 85
2.3.2.1 Electrode layer 85
2.3.2.2 Inductive coil layer 87
2.3.2.3 PCB layer 88
2.3.2.4 Other layers 89
2.3.3 Heat press process and heat formation process 90

Chapter 3 Results 93
3.1 Cell proliferation using implantable bioreactor 93
3.2 Bone regeneration results using bone

regeneration device 97
3.2.1 Radiological and histological examinations 97
3.2.2. Micro CT analysis 99

Chapter 4 Discussion 101
4.1 Implantable bone regeneration device for bone graft transplantation therapy 101
4.2 Selection of the electrical stimulation parameters 102
4.3 An alternative tissue engineering method of in situ stem cell therapy using intracorporeal cell culture 104
4.4 Transfer of electrical stimulation according to electrode design of bioreactor 106
4.5 Bone regeneration effect on combined treatment of electrical stimulation and 108
4.6 Potential for chronic bone substitute of LCP-based bone regeneration device LCP 110
Chapter 5 Conclusion 113

References 114

Abstract in Korean 121

List of Figures

Figure 1.1 Configuration of electrochemical cell 2
Figure 1.2 A conceptual diagram of movement and accumulation of electron according to increase of electron energy in electrode 4
Figure 1.3 Two charge transfer process at electrode/electrolyte interface. 5
Figure 1.4 A equivalent circuit model of electrode/electrolyte interface 6
Figure 1.5 Structure of cellular membrane and ion distribution across transmembrane 8
Figure 1.6 Structure of lipid bilayer 9
Figure 1.7 Equivalent circuit of plasma membrane 17
Figure 1.8 Thevenin equivalent circuit of the model in figure 1.7 18
Figure 1.9 Equivalent circuit when current is applied from

outside of cell 18
Figure 1.10 Applied current pulses and corresponding changes of transmembrane potential 19
Figure 1.11 Equivalent circuit of plasma membrane with reflection of active ion channels..... 20
Figure 1.12 Schematic of gating mechanism of voltage gated ion channel..... 21
Figure 1.13 Schematic of gating mechanism of ligand-gated ion channel..... 23
Figure 1.14 Ion channel gating mechanism of sea urchin sperm 24
Figure 1.15 Schematics of two gating models of mechanosensitive ion channel 26
Figure 1.16 Gating mechanism of channelrhodopsin..... 29
Figure 1.17 An example of gating mechanism of temperature sensitive ion channel..... 31
Figure 1.18 Feature of action potential..... 33
Figure 1.19 Equivalent circuit model of cell membrane including voltage gated ion channel 35
Figure 1.20 Transient change of ionic conductance of voltage-gated sodium channel and potassium channel..... 35
Figure 1.21 Intracellular calcium pathways 38
Figure 1.22 Cellular pathways and cellular process regulated by electrical stimulation in osteoblast.... 40
Figure 1.23 An early direct current stimulator for bone regeneration 43
Figure 1.24 Bone regeneration device of Biomet and schematic of application of the device to bone fracture..... 47
Figure 1.25 Crystal unit structure of LCP..... 51
Figure 2.1 Design of the bioreactor chamber..... 55
Figure 2.2 Feature of the stimulation chip bonded on the PCB..... 56
Figure 2.3 Three types of packaging molds used in current generator device 57
Figure 2.4 A feature of the packaged PCB with silicone elastomer..... 59
Figure 2.5 A schematic of bioreactor that uses titanium electrode..... 60

Figure 2.6 Bioreactor chamber and titanium electrode 61
Figure 2.7 The entire feature of bioreactor using titanium electrode..... 62
Figure 2.8 A schematic of the bioreactor using a polyimide electrode..... 62
Figure 2.9 Electrode part of the polyimide electrode 63
Figure 2.10 The setting of polyimide electrode into the bioreactor chamber 64
Figure 2.11 The entire feature of bioreactor using polyimide electrode 64
Figure 2.12 The process of cell proliferation experiment using bioreactor..... 68
Figure 2.13 The entire feature of bone regeneration device 71
Figure 2.14 The entire process of bone regeneration experiment..... 79
Figure 2.15 A conceptual art of LCP based implantable bone regeneration device 83
Figure 2.16 The entire process of producing LCP based bone regeneration device 84
Figure 2.17 The feature of the shadow mask 86
Figure 2.18 The produced electrode layer 86
Figure 2.19 The feature of the inductive coil layer..... 87
Figure 2.20 The feature of the inductive coil layer..... 88
Figure 2.21 PCB layer and wire bonded chip on the layer..... 89
Figure 2.22 LCP layers. Cover layer, bottom layer, dummy layer and adhesion layer in sequence 89
Figure 2.23 The mold for heat press process..... 90
Figure 2.24 The mold for heat formation process..... 91
Figure 3.1 Cell proliferation result of the in vivo cell culture using the implantable bioreactor with titanium electrodes 94
Figure 3.2 Cell proliferation result of the in vivo cell culture using the implantable bioreactor with polyimide electrode..... 95
Figure 3.3 Scaled-up features of adhered hMSCs on the collagen sponges..... 96
Figure 3.4 Total RNA extraction results of cell proliferation experiments using bioreactor 96
Figure 3.5 The illustration of rabbit mandible defect and radiological and histological images

of group 1, 2, 3 98
Figure 4.1 Concept of the conventional tissue regeneration therapy using *in vitro* cell culture and the intracorporeal cell culture..... 106
Figure 4.2 The current pathway in the bioreactor using titanium electrodes 108
Figure 4.3 The conceptual process for the different proliferation and differentiation of stem cells 110

List of Tables

Table 1.1 Nernst potentials and ion concentrations of some ions in neuron 13
Table 1.2 Family, location and gating mechanism of representative mechanosensitive channels.....26
Table 1.3 Temperature sensing range, location and nonthermal agonists of representative temperature sensitive ion channel 30
Table 1.4 FDA approved conventional bone regeneration devices using electrical stimulation.....45
Table 3.1 Evaluation and summery of the micro CT analysis....100

Chapter 1 Introduction

1.1 Regulation of cellular process through electrical stimulation

Neural prosthetic devices including artificial retina and cochlear implant, neuro modulation devices such as deep brain stimulation device, cell culture systems and tissue regeneration devices using electrical stimulation regulate action of nerve system and modulate cellular process through electrical stimulation [1−5]. Electrical stimulation which can be applied in forms of constant voltage/current or pulsed voltage/current, affects living body through electrode that mediates hardware such as voltage/current source and liveware such as neuron and tissue [6]. The hardware, the liveware and the electrode comprise electrochemical cell in figure 1.1 [7]. Electrochemical cell is a system that more than a pair of electrodes which are connected to power supply inserted into electrolyte. The each of electrodes acts cathode and anode. If current or voltage is generated by power supply of electrochemical cell, oxidation occurs at the anode and reduction occurs at the cathode. At this moment, oxidation current generated by oxidation at the anode has a same level with reduction current generated by reduction at the cathode. And a current which has same level of the oxidation current and reduction current flows through power supply and electrolyte between the anode and the cathode. The current

from electron and negative ion forms a closed loop. And the current flows a circuit of electrochemical cell when tracing flow of electron and negative ion in electrochemical cell. A term of stimulating biological tissue using electric stimulation device means that to construct an electrochemical cell of electrode, tissue and stimulation device, and to make the current flow each component forming a closed loop. The current flows forming a closed loop modulate cellular process. In this chapter, when electrical stimulation is generated from electrical stimulation device, how does a charge transfer to liveware and how does the liveware sense this charge flow and modulate cellular process will be demonstrated.

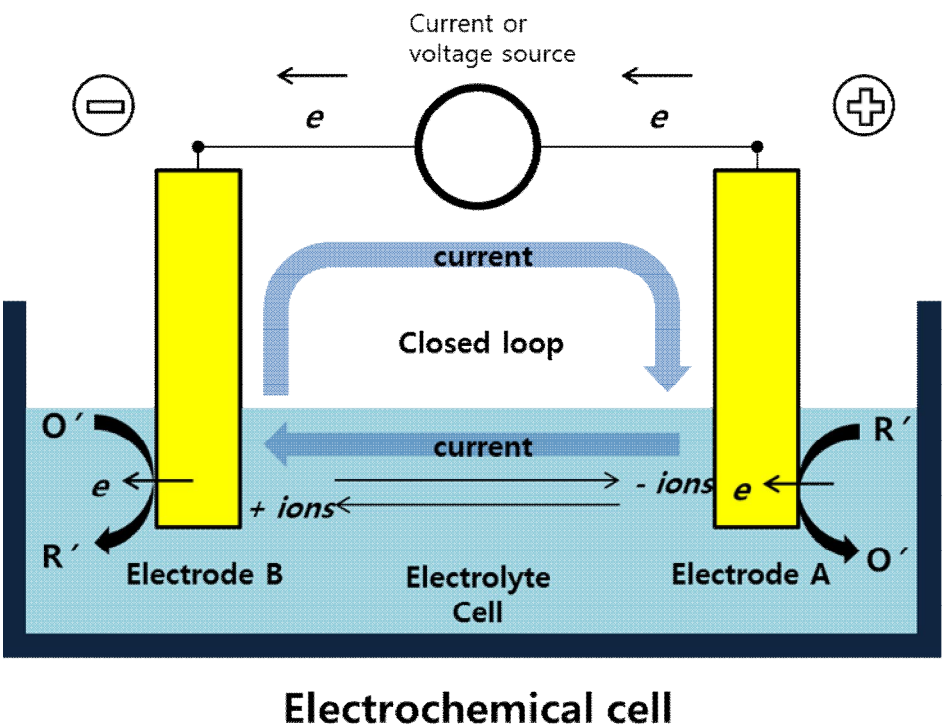

Figure 1.1 Configuration of electrochemical cell

1.1.1 Charge transfer at interface of electrode /electrolyte

When electricity is generated from power source of electrical device, current flows in a closed loop circuit consisted of electrode, tissue and power source. Current is a flow of charge. When a charge moves to electrode, energy of electron rises. The energy of electron rise when a potential of electrode increases to negative direction. Figure 1.2 demonstrates a process that movement and accumulation of electrons according to change of the energy of electron. A movement tendency of electron from electrode to electrolyte can be expected by comparing electron energy of electrode and compound in electrolyte. If Fermi level of electron in electrode is lower than highest occupied molecular orbital (HOMO) of compound in electrolyte, movement of electron from electrode to electrolyte – oxidation is possible. By contrast, Fermi level of electron in electrode is higher than lowest unoccupied molecular orbital (LUMO) of compound in electrolyte, movement of electron from electrolyte to electrode – reduction is possible.

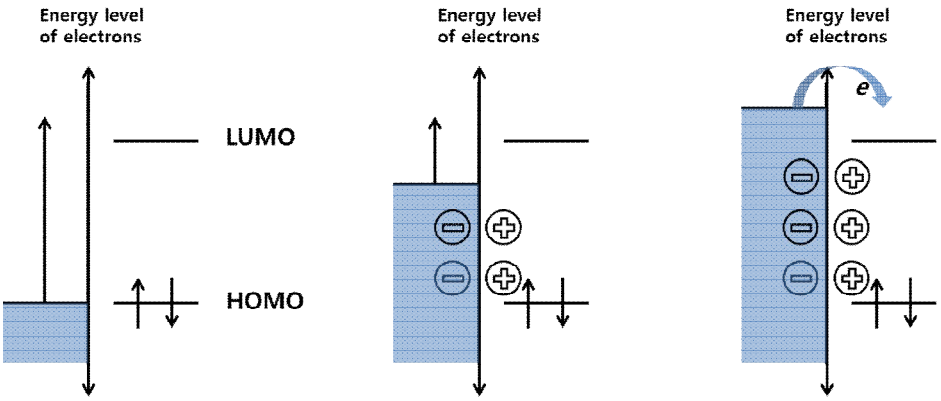

Figure 1.2 A conceptual diagram of movement and accumulation of electron according to increase of electron energy in electrode [7].

When electron transfers to electrolyte, electron transfers by capacitive process and faradaic process. Figure 1.3 demonstrates how the two processes occur in electrode and deliver electron. If negative potential or negative current applied in electrode, electrons move to electrode and electron energy increases. The electrons accumulate in the electrode and the electron energy increase continuously until the electron energy reaches to level of LUMO because electrons can transfer from electrode to electrolyte when the electron energy is higher than LUMO of electrolyte thermodynamically. At that moment, to maintain charge neutrality, cations from electrolyte move to electrode and form an electric double layer of 10~100 Å thickness at the surrounding of electrode. The electrons accumulate until the electron energy reach to LUMO level of compound in electrolyte. Therefore the electric double layer acts as a capacitor. The current which flows with charging electric double layer is called to be a capacitive current or

a double layer charging current. When a capacitive current flows, a same amount of displacement current arises by ions in electrolyte.

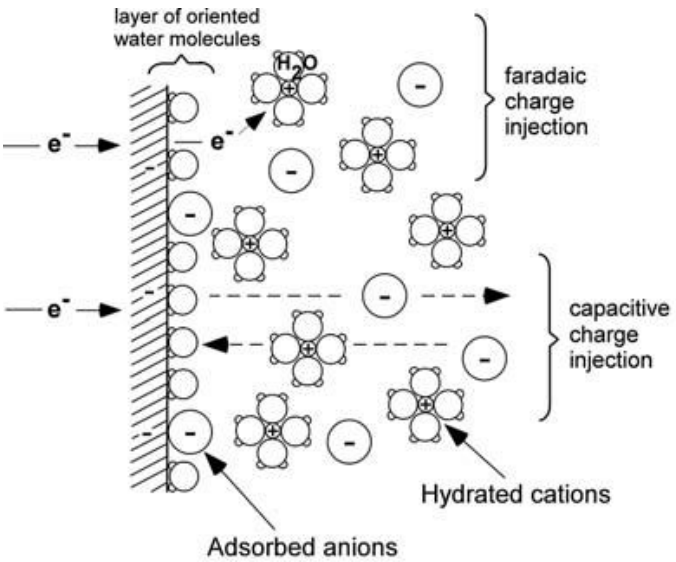

Figure 1.3 Two charge transfer process at electrode/electrolyte interface. [8]

Faradaic current is a current from electron transfer by chemical process when the electron energy in electrode exceeds LUMO level of compound in electrolyte. Amount of faradaic current is affected by speed of mass transfer and chemical reaction because the faradaic current arises from reduction/oxidation reaction between a surface of metal electrode and electrolyte.

From a fact that the charge transfer is conducted by the two processes at electrode and electrolyte interface, we can know a process that the current generated from a power supply device is transduced a summation of faradaic current and double layer charging current at electrode/electrolyte interface. The

electrode/electrolyte interface can be modeled in equivalent circuit model as figure 1.4, because the charge transfer is generated at the electrode/electrolyte interface. In this model, a capacitor demonstrates a charge of electric double layer, faradaic impedance means charge transfer and mass transfer which make chemical reaction. Otherwise, electrochemical reaction occurs in several hundred micro meters around electrode, so electron transfer from faradaic process does not be transfer to a bulk area in where a tissue should be stimulated is located.

At electrode/electrolyte interface, there is current from electron transfer and displacement current due to the two charge transfer processes. In bulk region a tissue and cells are affected by an ionic current which is same amount of the current from the two processes.

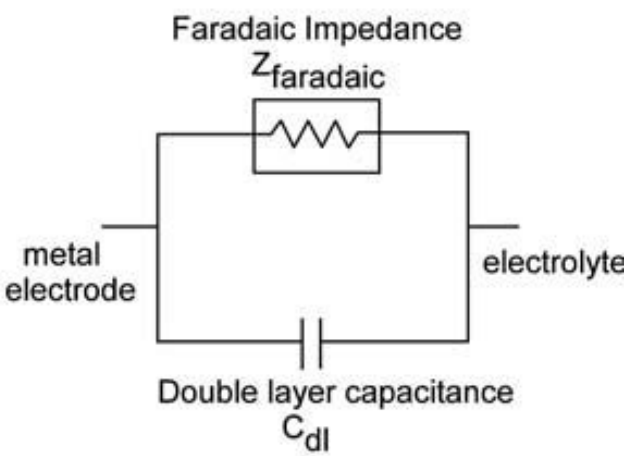

Figure 1.4 An equivalent circuit model of electrode/electrolyte interface [6]

1.1.2 Electrical equivalent circuit modeling of cellular membrane

It is necessary that electrical equivalent circuit modeling of cell to explore a modulation of electrical characteristic of cell due to ionic current applied from external electrical device. There is difference of amount of charge between interior of cell and extracellular space basically, and cells maintain a homeostasis in order that intracellular potential has a negative potential about −80 mV to −40 mV compared to extracellular potential [9]. Figure 1.5 demonstrates that which ions distribute in extracellular and intracellular spaces and which components are embedded in plasma membrane. Also it demonstrates electrical potential across plasma membrane that is transmembrane potential.

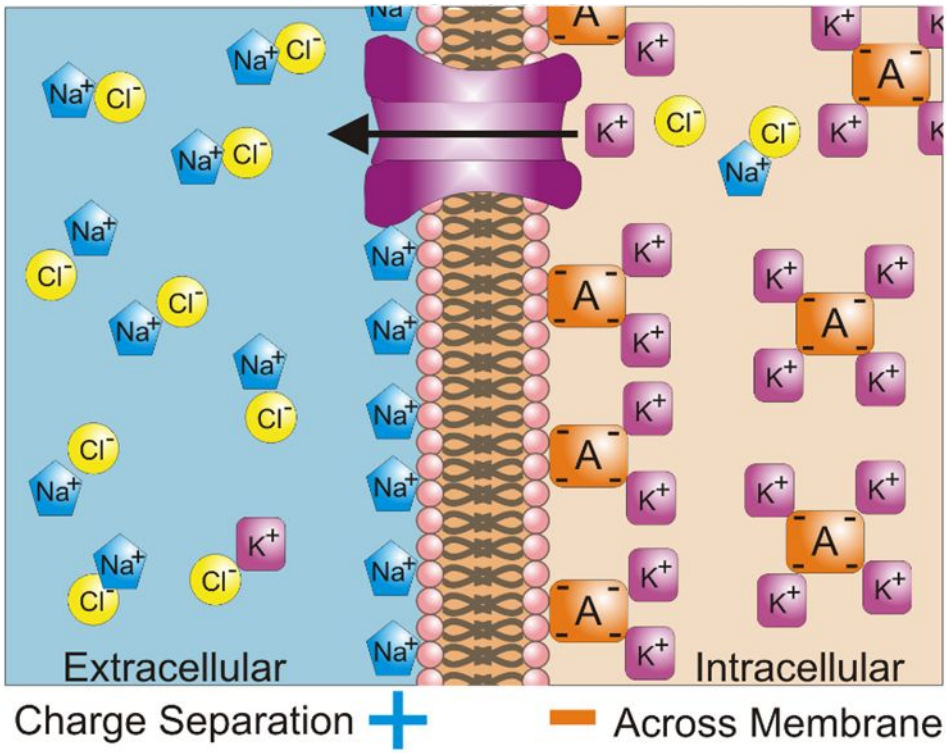

Figure 1.5 Structure of cellular membrane and ion distribution across plasma membrane [10]

In extracellular space, chloride and sodium ions are many compare to intracellular space. In intracellular space, potassium ions and anions such as amino acid are many compare to extracellular space. Separation of ion concentration across plasma membrane is possible through a special structure called a lipid bilayer. Figure 1.6 shows a structure of lipid bilayer that consists of plasma membrane.

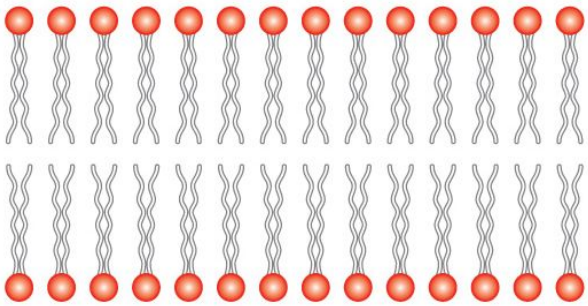

Figure 1.6 Structure of lipid bilayer [11]

Phospholipid consists of hydrophilic head and hydrophobic leg. A pair of phospholipid makes face to face each other with its hydrophobic leg and this pair of phospholipid comprises plasma membrane. Ions in extracellular and intracellular space cannot move across plasma membrane because two-dimensional structure of hydrophilic head of phospholipid comprise interface of intracellular and extracellular space and hydrophobic layer of phospholipid leg is located in a center of plasma membrane. Ion distribution in extra/intracellular space is separated and potential difference is generated according to existence of lipid bilayer. As mentioned above the potential of intracellular space is lower than the potential of extracellular space, but bulk region of extra/intra cellular space maintains charge neutrality. Most potential difference is applied to the plasma membrane. Anions and cations are arranged with the plasma membrane. The potential difference with extra/intra cellular space that is the potential which arise from accumulation of anions and cations across the plasma membrane is called a transmembrane potential [12]. Ions cannot move through plasma membrane and

cation and anion accumulate according to transmembrane potential, plasma membrane has same characteristic of capacitor. Plasma membrane is modeled by capacitor and capacitance per unit area of plasma membrane is reported as 1 μF/cm^2 [13].

Plasma membrane has another special cellular structure ion channel which allows ion movements across plasma membrane. Ion channel consists of several units of proteins. Each ion channel is named after ions that ion channel pass through. To maintain homeostasis, separation of ion concentration across plasma membrane regulates transmembrane potential with ion channels. The existence of ion channel which allows special ion to pass through plasma membrane and separated ion concentration make electrical potential difference at each ion channel. And the potential difference from each ion channel affects transmembrane potential. Before exploring effects of each ion in intra/extra cellular space on to the transmembrane potential, let's derive a general equation of specific ion channel effect on transmembrane potential. After that, the effect of every ion on the transmembrane potential can be derived by expanding the equation of specific ion to case of every ion. For example, let's consider an ion channel that only pass potassium ion. There is difference of ion concentration of potassium at across of the plasma membrane. Potassium ion diffuses from intra cellular space in which has higher potassium ion concentration to extra cellular space in which has lower potassium ion concentration. This diffusion is a current because ion diffusion, the current is called a diffusion current of potassium. The diffusion current can be explained

following equation by Fick's first law [9].

$$J(\text{diffusion}) = -D\frac{d[I]}{dx} \qquad (1.1)$$

Furthermore, due to potential difference of transmembrane potential, electric field is formed at across plasma membrane. Ions move by this electric field. The current formed by the electric field from transmembrane potential is called a drift current. Drift current can be explained following equation by Ohm's law [9].

$$J(\text{drift}) = -\mu Z[I]\frac{dv}{dx} \qquad (1.2)$$

It can be considered a dynamic equilibrium state in that a summation of drift current and diffusion current is zero at potassium channel. In this condition, a summation of equation 1.1 and 1.2 is zero, and it derives equation 1.3

$$J(\text{ion}) = J(\text{diffusion}) + J(\text{drift}) = -D\frac{d[I]}{dx} - \mu Z[I]\frac{dv}{dx} = 0$$

(1.3)

Then using Einstein equation (equation 1.4), equation 1.5 can be derived [9].

$$D = \frac{KT\mu}{q} \quad (1.4)$$

$$dv = -\frac{KT}{qZ[I]}d[I] \quad (1.5)$$

Then solving integral from extra cellular region to intra cellular region (equation 1.6), equation 1.7 can be derived.

$$\int_{v_o}^{v_i} dv = -\frac{KT}{qZ}\int_{[I]_o}^{[I]_i}\frac{d[I]}{[I]} \quad (1.6)$$

$$E = \frac{KT}{qZ}ln\frac{[I]_o}{[I]_i} \quad (1.7)$$

Equation 1.7 is called to be a Nernst equation and corresponding ion makes a dynamic equilibrium state when transmembrane potential is Nernst potential of that ion [12]. That is to say, in case that ion separation due to selective permeable membrane is occurred and there is only one ion channel for corresponding ion, that ion cannot make dynamic equilibrium state and undergo diffusion and drift through ion channel until the Nernst potential. The separation of ion concentration and existence of ion channel drive the potential across ion channel. Therefore ion channel can be modeled as a battery that has electromotive force as much as Nernst potential

[12]. Also the ion channel is passage of ion, so this is modeled as a conductance [9].

Furthermore Nernst equation of specific ion can be apply to every ion that has separated ion concentration and ion channel, each ion can be modeled as a series circuit of battery and conductance [9]. Of course every ion has different ion concentration each other, so Nernst potential of each ion – potential that ion drives is different each other. Table 1.1 shows some Nernst potentials according to ion distribution in neuronal cell [12].

Table 1.1 Nernst potentials and ion concentrations of some ions in neuron.

Ion	Cytoplasm (nM)	Extracellular Fluid (mM)	Nernst Petential (mV)
Potassium	400	20	−74
Sodium	50	440	55
Chloride	52	560	−60

Cells maintain transmembrane potential at resting state. General transmembrane potential is differ to Nernst potentials of each ion. This means that each ion undergo diffusion and drift continuously and maintain dynamic equilibrium state at given transmembrane potential. Therefore according to space charge neutrality, cathodal current and anodal current flow across plasma membrane should be same in resting state [9].

$$\sum J(\text{anion}) = \sum J(\text{cation}) \quad (1.8)$$

On the other hand, in resting state, for the transmembrane potential is constant so electric field across plasma membrane is also constant.

$$\frac{dv}{dx} = \frac{V}{\delta} \quad (1.9)$$

Then equation 1.9 is substituted into equation 1.8, and introducing a concept of permeability shown in equation 1.10, equation 1.11 is derived [9].

$$(P = \frac{\mu KT}{\delta}, Z = 1) \quad (1.10)$$

$$J(\text{ion}) = -D\frac{d[I]}{dx} - \mu Z[I]\frac{dv}{dx} = -\frac{KT}{q}\mu\frac{d[I]}{dx} - \mu Z[I]\frac{V}{\delta} = \frac{-Pq}{KT}V[I] - P\delta\frac{d[I]}{dx}$$

(1.11)

Permeability is proportional to mobility of ion. It expresses how each ion diffuses or drifts easily. This is related to conductance of each ion channel directly. A large permeability or a large conductance means that corresponding ion channel can pass ion easily. If there are many ion channels or many ion channels are

open, permeability and conductance are large. Now let's change equation 1.11 to equation 1.12 to make integration. Then solving integral from intra cellular region to intra cellular region (equation 1.13), equation 1.14 can be derived.

$$dx = \frac{d[I]}{\frac{-J}{P\delta} - \frac{qV[I]}{KT\delta}} \quad (1.12)$$

$$\int_0^{\delta} dx = \int_{[I]_i}^{[I]_o} \frac{d[I]}{\frac{-J}{P\delta} - \frac{qV[I]}{KT\delta}} \quad (1.13)$$

$$\delta = -\frac{KT\delta}{qV} \ln \frac{\left(\frac{J}{P\delta} + \frac{qV[I]_o}{KT\delta}\right)}{\left(\frac{J}{P\delta} + \frac{qV[I]_i}{KT\delta}\right)} \quad (1.14)$$

Equation 1.15 can be derived from arranging equation 1.14, from this equation, equations of cathodal current and anodal current of each ion.

$$e^{-\frac{qV}{KT}} = \frac{\frac{J}{P\delta} + \frac{qV[I]_o}{KT\delta}}{\frac{J}{P\delta} + \frac{qV[I]_i}{KT\delta}} \quad (1.15)$$

$$J(cation) = \frac{qVP}{KT\delta}\left(\frac{[I]_o - [I]_i e^{-\frac{qV}{KT}}}{e^{-\frac{qV}{KT}} - 1}\right) \quad (1.16)$$

$$J(anion) = \frac{qVP}{KT\delta}\left(\frac{[I]_o e^{-\frac{qV}{KT}} - [I]_i}{e^{-\frac{qV}{KT}} - 1}\right) \quad (1.17)$$

Then substitution of equation 1.16 and 1.17 to equation 1.8 and solving for every cation and anion equation 1.18 is derived.

$$\sum_n^m P_{I_n^+}\left([I_n^+]_o - [I_n^+]_i e^{-\frac{qV}{KT}}\right) = \sum_j^k P_{I_j^-}\left([I_j^-]_o e^{-\frac{qV}{KT}} - [I_j^-]_i\right) \quad (1.18)$$

This equation can be change to equation 1.19 and solving for V, finally equation 1.20 is derived. This equation is called a Goldman's equation [14].

$$e^{-\frac{qV}{KT}} = \frac{\sum_n^m P_{I_n^+}[I_n^+]_o + \sum_j^k P_{I_j^-}[I_j^-]_i}{\sum_n^m P_{I_n^+}[I_n^+]_i + \sum_j^k P_{I_j^-}[I_j^-]_o} \quad (1.19)$$

$$V = \frac{KT}{q}\ln\frac{\sum_n^m P_{I_n^+}[I_n^+]_o + \sum_j^k P_{I_j^-}[I_j^-]_i}{\sum_n^m P_{I_n^+}[I_n^+]_i + \sum_j^k P_{I_j^-}[I_j^-]_o} \quad (1.20)$$

From Goldman's equation, it is considerable that permeability and conductance of each ion, a condition of ion channel in plasma membrane, and ion concentration affect to formation of transmembrane potential of cell directly. When conductance of specific ion channel is large, the transmembrane potential

converges to Nernst potential of corresponding ion. The transmembrane potential of cell is determined by separation of ion concentration for maintaining cell homeostasis and distribution or gating condition of ion channel. Now, using components that determine transmembrane potential of cell, equivalent circuit model of plasma membrane is shown in figure 1.7

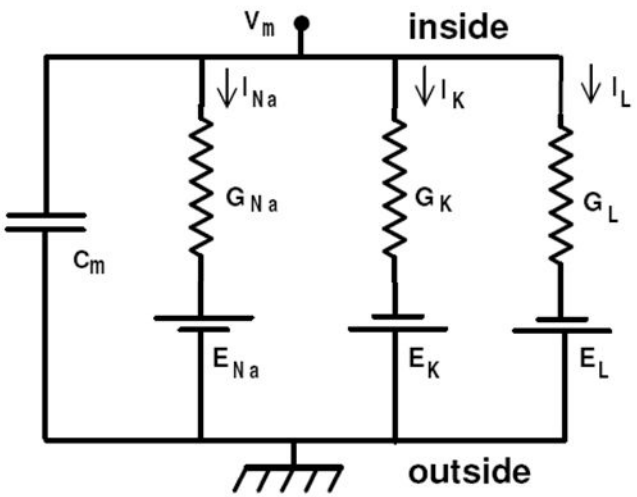

Figure 1.7 Equivalent circuit of plasma membrane [9]

The capacitor demonstrates lipid bilayer of plasma membrane, the series circuit of the battery and the conductance demonstrates each ion channel. The equivalent circuit can be simplified in Thevenin equivalent circuit.

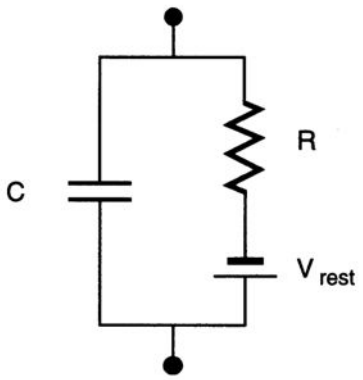

Figure 1.8 Thevenin equivalent circuit of the model in figure 1.7 [9]

Otherwise, ionic current of extra cellular space flows into cell and electrolyte. This can be modeled as current source is connected to series circuit of cytoplasm resistance and transmembrane circuit. Figure 1.9 demonstrates entire equivalent circuit for this situation.

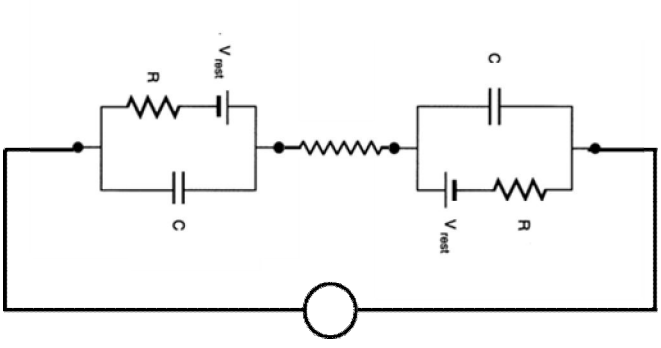

Figure 1.9 An equivalent circuit when current is applied from outside of cell.

From this circuit model, change of transmembrane potential can be calculated in case of applying current pulse. Current applied to cell is given as equation 1.21, and if amplitude of current pulse is I_i, and

duration of current pulse is t_i, change of transmembrane potential is derived as equation 1.22. Figure 1.10 demonstrates changes of transmembrane potential when current pulses applied cell membrane.

$$I = \frac{V_m - V_{rest}}{R} + C\frac{dV_m}{dt} \quad (1.21),$$

$$V_m = V_{rest} + RI_i\left(1 - e^{-\frac{t}{RC}}\right)u(t) - RI_i\left(1 - e^{-\frac{t-t_i}{RC}}\right)u(t - t_i)$$

(1.22) .

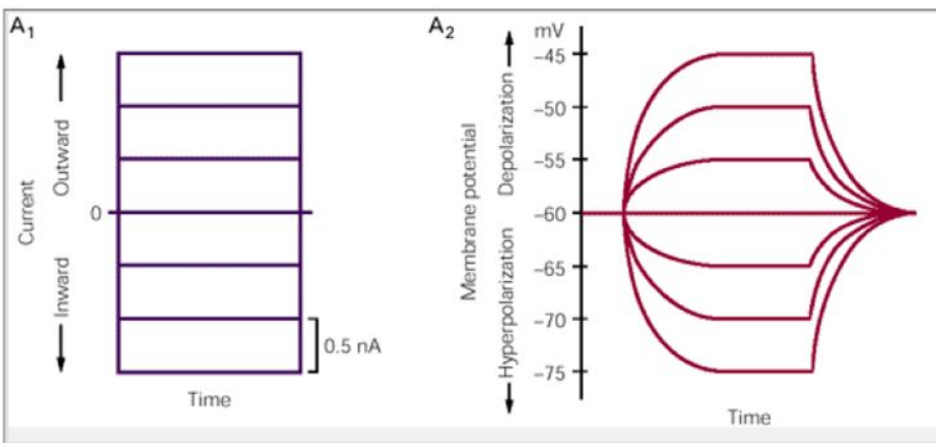

Figure 1.10 Applied current pulses and corresponding changes of transmembrane potential [13].

1.1.3 Gating mechanisms of ion channels

In former section explained that ion channel is modeled as a conductance in equivalent circuit modeling. Ion channel that passes

only specific ion is named as specific ion channel. And ion channel that passes ion regardless of ion kind is named as non-specific ion channel [12]. Also there are passive ion channels which are open always otherwise there are ion channels that have various gating mechanisms. These gating channels open and close its channel according to various stimulations applied on plasma membrane. Ion conductance and permeability of plasma membrane change according to gating of ion channel. From this, equivalent circuit of ion channel is demonstrated as variable conductance and battery. Furthermore, these gating channels which are activated by specific mechanism such as electrical stimulation allow the modulation of cellular processes. In this section, various gating mechanisms of active ion channels are demonstrated.

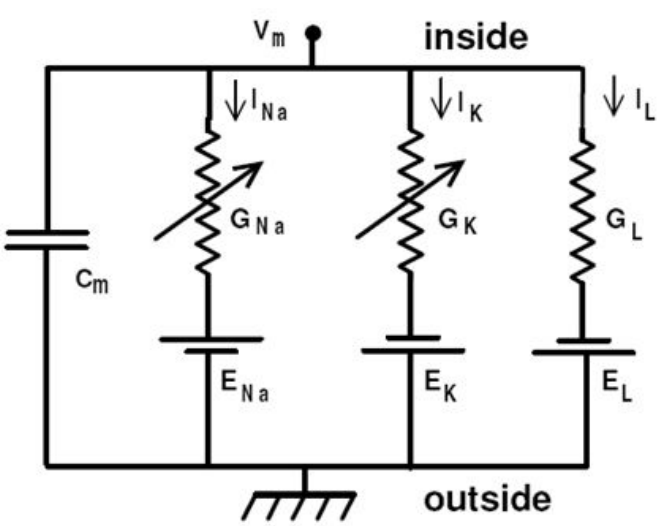

Figure 1.11 Equivalent circuit of plasma membrane with reflection of active ion channels. [9]

1.1.3.1 Voltage-gated ion channel

Voltage-gated ion channel closes when transmembrane potential maintains resting potential and opens when transmembrane potential change is occurred by hyperpolarization or depolarization as showed in figure 1.12. This channel is named by the type of passing ion for example of voltage-gated sodium channel, potassium channel, calcium channel and so on. In general, the gating of voltage gated ion channels is regulated by change of transmembrane potential, and it is affected by pH or condition of extra cellular space also [15].

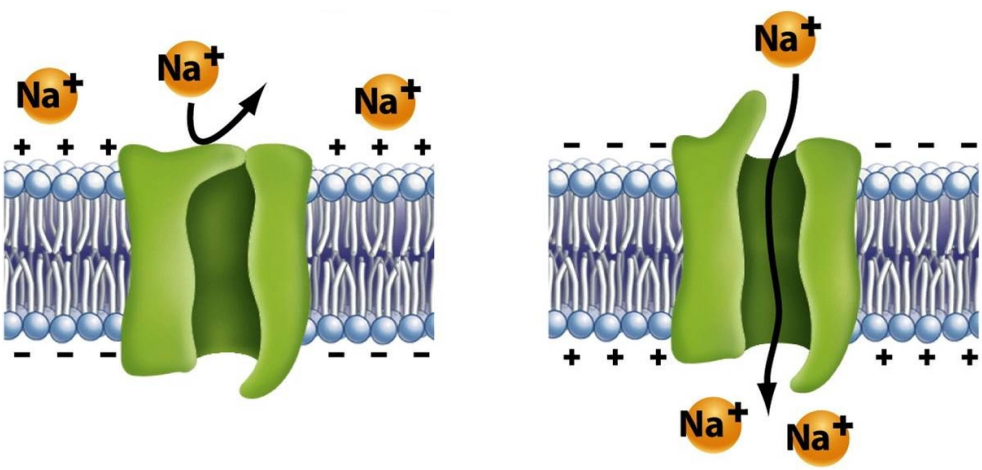

Figure 1.12 Schematic of gating mechanism of voltage gated ion channel [15]

1.1.3.2 Ligand-gated ion channel

This channel is gated when specific ligand which acts as chemical messenger such as neurotransmitter binds to receptor protein of ion channel. Especially the channel which is gated by binding at extracellular surface is referred as ligand-gated. Also according to ligand material, the name of channel is determined. This channel reacts to ligand basically, and its gating is affected by channel blocker, ion concentration, membrane potential or enzyme. Representative types of this channel include nicotinic Ach receptor channel (nAchR channel), ionotropic glutamate receptor channel, ATP-gated P2X receptor channel, GABA receptor channel.

This channel classified into three kinds of super family according to absence of evolutional relationship and each family has structural difference [12]. The family separated to Cys-loop receptor, ionotropic glutamate receptor and ATP-gated P2X receptor. Cys-loop receptor channel is named by possession of a specific loop structure between amino acid of Cystein. This super family has five of sub-unit structure. The channels which are gated by neurotransmitter including serotonin, Ach, glycine, GABA belong to this super family. In contrast with Cys-loop receptor channel, glutamate receptor channel consists of four of sub-unit. This channel is activated by glutamate only. ATP-gated P2X receptor channel is activated by reaction with ATP and its sub-unit structure is not known as well. Figure 1.13 demonstrates schematic of gating mechanism of ligand-gated ion channel.

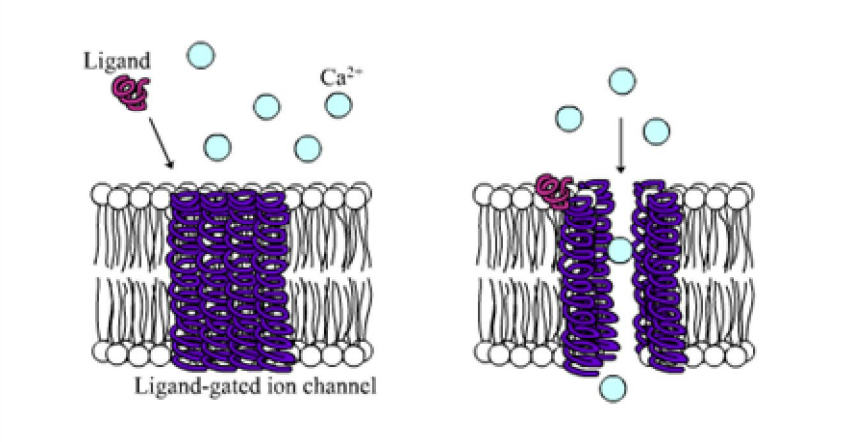

Figure 1.13 Schematic of gating mechanism of ligand-gated ion channel [16]

1.1.3.3 Second messenger gated ion channel

When primary transmitter receptor is activated by ligand such as neurotransmitter, intracellular second messenger is generated. Then second messenger gated ion channel is gated by corresponding second messenger. This channel uses intra cellular ATP, PIP, G-protein, cAMP and cGMP as second messengers. Figure 1.14 is an example of this channel. This figure demonstrates ion channel gating mechanism of sea urchin sperm [17]. When ligand binds to guanylyl cyclase (GC), second messenger cGMP is generated. Then cGMP activated cyclic nucleotide gated potassium channel. Activation of potassium channel makes hyperpolarization of cell membrane. Otherwise cGMP undergoes hydrolysis by phosphodiesterase (PDE), then change into GMP. The GMP blocks action of GC. According to hyperpolarization of transmembrane

potential, hyperpolarization-activated and cyclic nucleotide-gated (HCN) sodium channel is activated. Intracellular cAMP participates to activation of HCN sodium channel also. Activated HCN sodium channel depolarizes membrane potential and drives to activate voltage-gated calcium channel. After activation of calcium channel, intracellular calcium concentration increases and cellular pathway is initialized. This cellular pathway modulates turning of sperm. After this event, intracellular calcium concentration is back to resting level by Ca^{2+}/Na^{+} exchanger. In addition to this example there are many complex mechanisms for this channel.

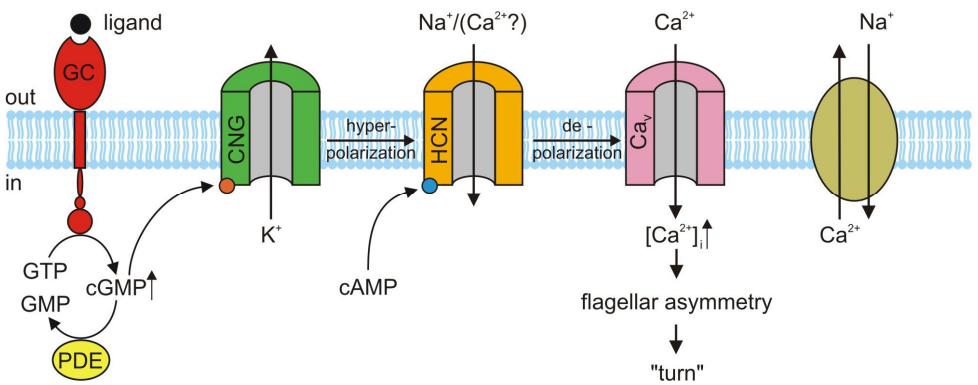

Figure 1.14 Ion channel gating mechanism of sea urchin sperm [17]

1.1.3.4 Mechanosensitive ion channel

Every cell reacts to mechanical stimulation and transduces mechanical stimulation into electrical signal through mechanosensitive ion channel. Mechanosensitive channel is related

with not only hearing and touch but also various body function including blood pressure, cell swelling and musculoskeletal development. This channel has various types of structure, function and gating mechanism. Also every possible mechanism of signaling pathway that elicit electrical signal has been reported [18]. That is there is a channel which is regulated channel gating with membrane potential or agonist. Also there is a channel which gates ion flow directly or using second messenger. Table 1.2 shows family, its location and gating mechanism of representative mechanosensitive channels.

Mechanosensitive ion channel has various kinds and structure, but they share important gating mechanism that the channel which consists of proteins is activated by mechanical stimulation and makes a pore of channel. Gating mechanism of mechanosensitive ion channel has following two models. 1) Lipid bilayer tension model (stretch model): In this model, plasma membrane changes its structure by lipid bilayer tension, then shape change of plasma membrane gates ion channel that embedded on plasma membrane. MSC family of bacteria uses this model typically [19]. 2) Tether model: In this channel, protein unit of mechanosensitive channel makes a direct connection to extra cellular matrix or cytoskeleton with chain structure. When external mechanical stimulation is occurred, a relative displacement between ion channel and extra cellular matrix or cytoskeleton is generated and this relative displacement regulated channel gating. Hair cell is a typical cell using this model [20]. Figure 1.15 demonstrates schematics of the

two models.

Table 1.2 Family, location and gating mechanism of representative mechanosensitive channels [21]

Channel	Source	gating mechanism	physiological role
MscL	bacteria	lipid bilayer	turgor regulation and cell growth
MscS	bacteria	lipid bilayer	turgor regulation and cell growth
MscMJ	archaea	lipid bilayer	turgor regulation
MEC4	C. elegans	tether	touch
TRPY	fungi	lipid bilayer	turgor regulation
TRECK-1	mammalian	lipid bilayer	resting membrane potential
TRP-1	hair cell	tether	hearing

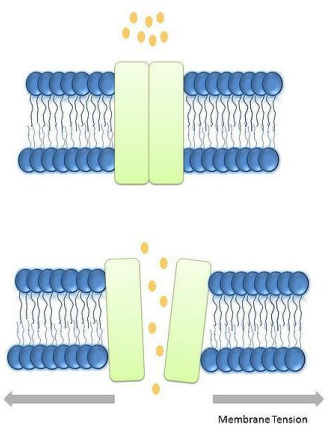

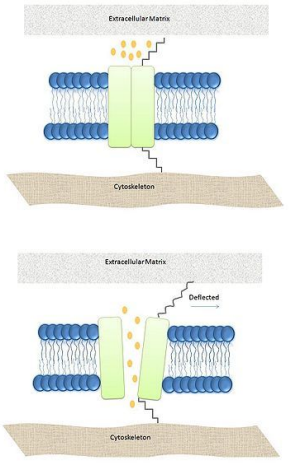

Figure 1.15 Schematics of two gating models of mechanosensitive ion channel [21]

1.1.3.5 Light sensitive ion channel

Channelrhodopsin is a representative light-sensitive ion channel. This ion channel is discovered in Chlamydomonas microalgae [22]. Channelrhodopsin is a sub family of rhodopsin. Rhodopsin is a visual pigment which lies on free-floating disc membrane inside of outer segment of a photoreceptor cell. This consists of a covalent complex of a large protein, opsin and a small ight-absorbing compound, retinal. According to type of rhodopsin, a wavelength of light absorbed by retinal is different. In opsin, a binding site exists for retinal, and the retinal fits snugly into the binding site of the opsin. When light stimulation is introduced, the retinal absorbs the light and undergoes molecular structural change. Then opsin cannot bind the retinal which is transformed by structural change and the released retinal initiates a cascade event which modulates membrane potential. The retinal stimulates a G-protein, and the stimulated G-protein activates a cGMP phosphodiesterase, then concentration of the cGMP in the photoreceptor cell decrease. The change of the cGMP concentration regulates a cGMP-gated ion channel, this ion channel participates depolarizing of membrane potential. This signal transfers to bipolar cell, ganglion cell and visual pathway [12]. While rhodopsin generates a second

messenger from light stimulation and regulates gating of ion channel, channelrhodopsin acts as an ion channel itself. Channel rhodopsin also has opsin and retinal structure. The retinal of rhodopsin binds and detaches to opsin, and the retinal of channel rhodopsin composes a pore of ion channel. The retinal of channelrhodopsin also absorbs different wavelength of light according to kind of channel. When the retinal of channelrhodopsin absorbs light of specific wavelength, the retinal undergoes conformational change. From this change, the ion channel is gated and membrane potential modulation is occurred. The conformational change of channelrhodopsin is very fast so the gating of channel is executed in several milliseconds. This channel acts as a non-specific ion Channelrhodopsin is sub familychannel. In figure 1.16, gating mechanism of channelrhodopsin is demonstrated.

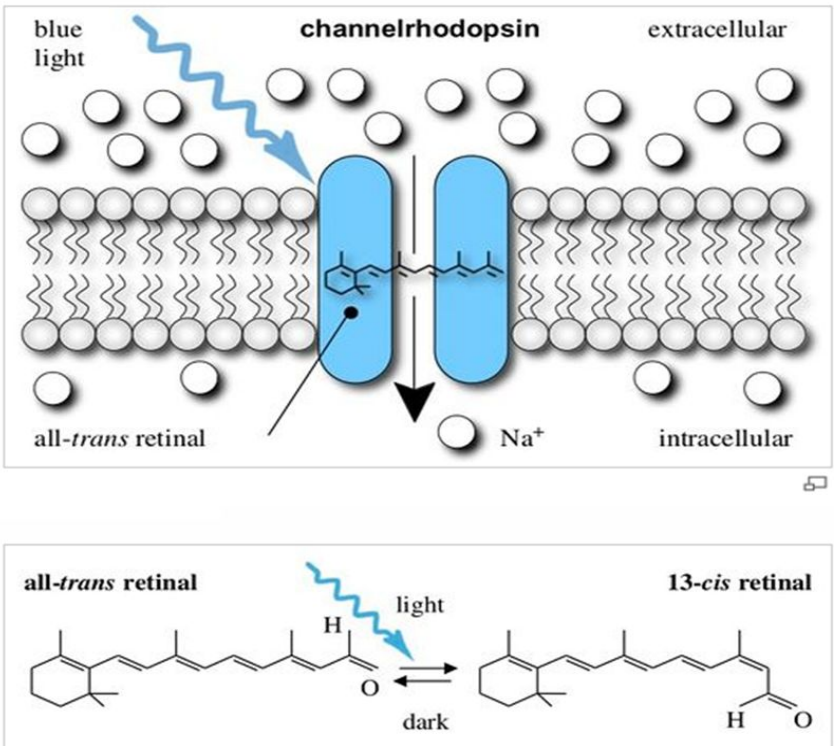

Figure 1.16 Gating mechanism of channelrhodopsin [22]

1.1.3.6 Temperature sensitive ion channel

Temperature sensitive ion channel is separated into a family of transient receptor potential (TRP) channel and non TRP channel [23]. In table 1.3, temperature sensing range, location and non-thermal agonists of some representative temperature sensitive ion channels are listed.

Table 1.3 Temperature sensing range, location and non-thermal agonists of representative temperature sensitive ion channel [24]

channel	temperature sensitivity	Location	Non-thermal agonists
TRPV1	>42℃	PNS, brain skin, spinal cord, tongue, bladder	capsaicin, lipoxygenase, acidic pH, resiniferatoxin, NADA, anandamide, EtOH allicin, camphor
TRPV2	>52℃	PNS, brain, skin, spinal cord	growth factors
TRPV3	>33℃	PNS, skin	camphor, 2-APB
TRPV4	27~42℃	kidney, PNS, skin, inner ear, brain, liver, heart, fat	hypotonic, phorbol esters
TRPM8	<25℃	PNS,	menthol, icilin, eucalyptol
TRPA1	<17℃	PNS, hair cell	cinnamaldehyde, mustard oil, allicin, icilin, etc.
TREK-1	cold	PNS, brain	membrane stretch, polyunsaturated fatty acids, intracellular pH
P2X3	warmth	PNS	ATP

Gating of temperature sensitive channel is regulated by various agonists except temperature. Nevertheless membrane potential of cell participates to channel gating. There are two models of gating mechanism for this ion channel, one is 2-state model of Voets [25],

and another is 8-state model of Brauch [26]. Suggested common gating mechanism of two models is that difference of activation energy due to temperature change causes conformational change of channel and channel gating by second messenger. In two models, a membrane potential and temperature change are main variables of gating mechanism. There are no established gating mechanisms of temperature sensitive channel. There are many hypotheses regarding the mechanism of channel gating. The hypotheses includes that ion channel has a pore turret and this turret is gated by temperature or amino acid which is connected to channel acts gating lever, or denaturation of protein due to heat modulates gating.

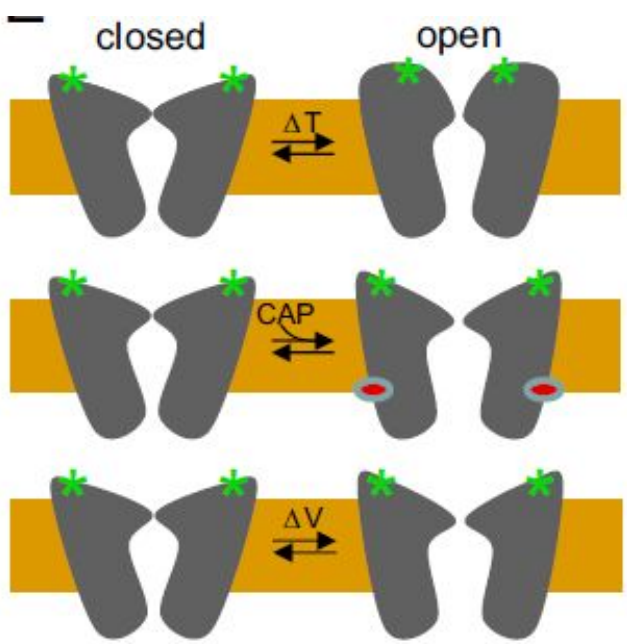

Figure 1.17 An example of gating mechanism of temperature sensitive ion channel [27]

1.1.4 Cellular processes generated by change of transmembrane potential

Electrical stimulation generated from power supply device transfers electric charge through faradaic process and non-faradaic process at electrode/electrolyte interface. The charge is transferred in the form of ionic current to cell membrane. The electrical equivalent model of a plasma membrane helps to know that how does a membrane potential change according to ionic current. The change of transmembrane potential affects to cellular process modulation directly or indirectly. Especially the change of transmembrane potential from electrical stimulation modulates important cellular processes regulating the gating of voltage-gated ion channels. There are two important cellular processes which are regulated by voltage-gated ion channel – generation of action potential and triggering intracellular second messenger signaling pathway.

1.1.4.1 Generation of action potential

Action potential is a short-lasting event that membrane potential increase rapidly then decrease rapidly as like as shown in figure 1.18 [28]. The action potential is generated in excitable cells only. The excitable cells that can generate action potential include neuron, muscle cell and endocrine cell [12]. The action potential takes an important role in cell to cell communication. When membrane

potential exceeds threshold potential, conductance change of voltage-gated ion channel is occurred. The action potential is generated by difference of transient change of ion channel conductance.

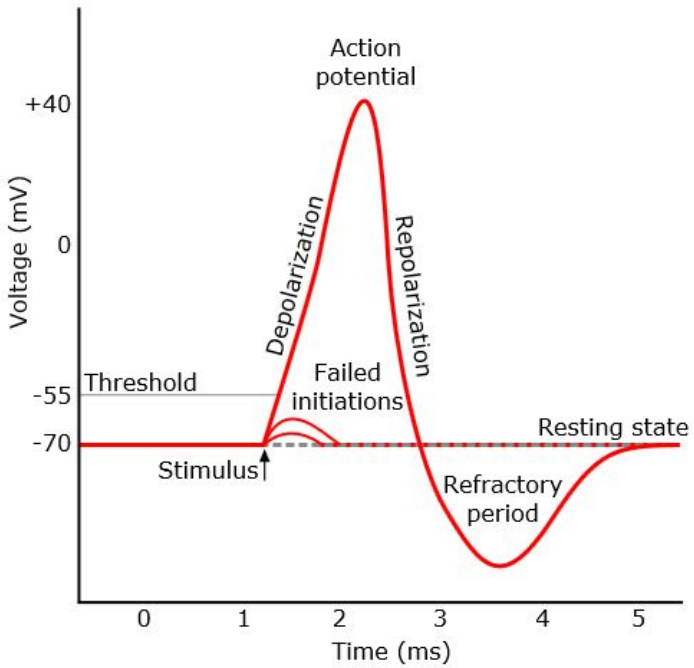

Figure 1.18 Feature of action potential [28]

As like as figure 1.19, voltage-gated ion channel can be modeled as a variable conductance. These conductances have a different tendency of conductance change when membrane potential exceed threshold potential. Figure 1.20 shows transient changes of ion conductance of each voltage-gated sodium channel and voltage-gated potassium channel. Also action potential shape when membrane potential exceed threshold potential is demonstrated. When transmembrane potential of a cell is depolarized by external

electrical stimulation and exceed threshold potential, a voltage-gated ion channel is activated. As shown in figure 1.20, the conductance change of voltage gated sodium channel is faster than the conductance change of a voltage gated potassium channel. Before activating of the potassium channel, a sodium ion channel is open and sodium ion current flows. This sodium current makes further depolarization of membrane potential. This relationship can be checked in Goldman's equation. When a sodium ion channel is activated, sodium ion conductance increases and membrane potential is driven to Nernst potential of sodium ion. Then the membrane potential depolarizes continuously and finally the membrane potential changes to positive potential. After that, the sodium channel is close and sodium current decreases rapidly. Then the voltage-gated potassium channel lately gated makes potassium current. As the sodium conductance decrease rapidly and the potassium conductance increase rapidly, the potassium current drives the membrane potential as the Nernst potential of potassium ion. During this event, the membrane potential hyperpolarized rapidly.

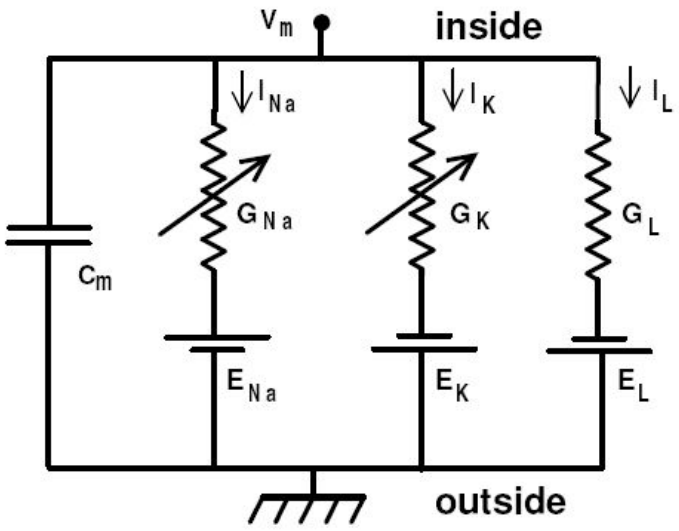

Figure 1.19 Equivalent circuit model of cell membrane including voltage gated ion channel

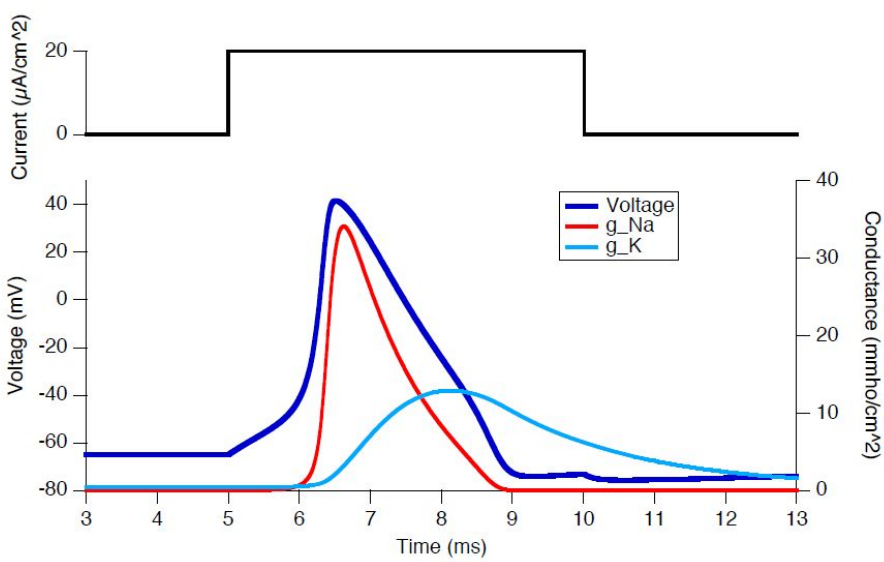

Figure 1.20 Transient change of ionic conductance of voltage-gated sodium channel and potassium channel [29]

1.1.4.2 Intracellular second messenger signaling pathway

Voltage-gated ion channel is gated by membrane potential then a primary cellular process, intracellular second messenger signaling pathway is triggered. It appears through gating a channel with changing the membrane potential and that channel transports ion that triggers intracellular pathway. The representative second messenger which regulates intracellular pathway through voltage-gated ion channel is a calcium ion. In resting state, the calcium ion concentration is very low about 100 nM compare to other ions. When the voltage-gated calcium channel is gated with membrane potential change, extracellular calcium flux into cytoplasm and secretion of calcium ion from intracellular calcium storage occurs. As a result intracellular calcium concentration increases by 100 times, then a various cellular processes regulated including action potential generation, secretion, proliferation, cell swelling, differentiation, transcription and synaptic transmission [30]. Figure 1.21 [31] demonstrates that intracellular calcium ion pathway cascade. With membrane potential increase the cell undergoes depolarization. Then the voltage-gated calcium channel is open and intracellular calcium concentration increases. The increased intracellular calcium binds intracellular ubiquitous calcium binding protein, calmodulin. The calmodulin bound with calcium activates serine/threonin phosphatase Calcineurin. The calcineurin

dephosphorylates transcription factor of NF-AT family, leads a translocation to cell nucleus. Then translocated NF-AT1 becomes a member of nuclear factor of activated T cell transcription. This complex roles primary action and the action involve gene transcription during immune reaction [32]. Furthermore the calmodulin with calcium activates calcium/calmodulin dependant protein kinase, CaMKI, CaMKII, CaMKIV and CaMKK. CaMKII and CaMKIV regulate gene transcription through several transcription factors including cAMP responsive element binding protein (CREB) [33]. Especially CREB is discovered its role for neuronal plasticity at brain and long-term memory formation [33]. CaMKI and CaMKIV phosphorylate Histone deacetylases (HDAC4, HDAC5, HDAC7) and regulates gene transcription [34].

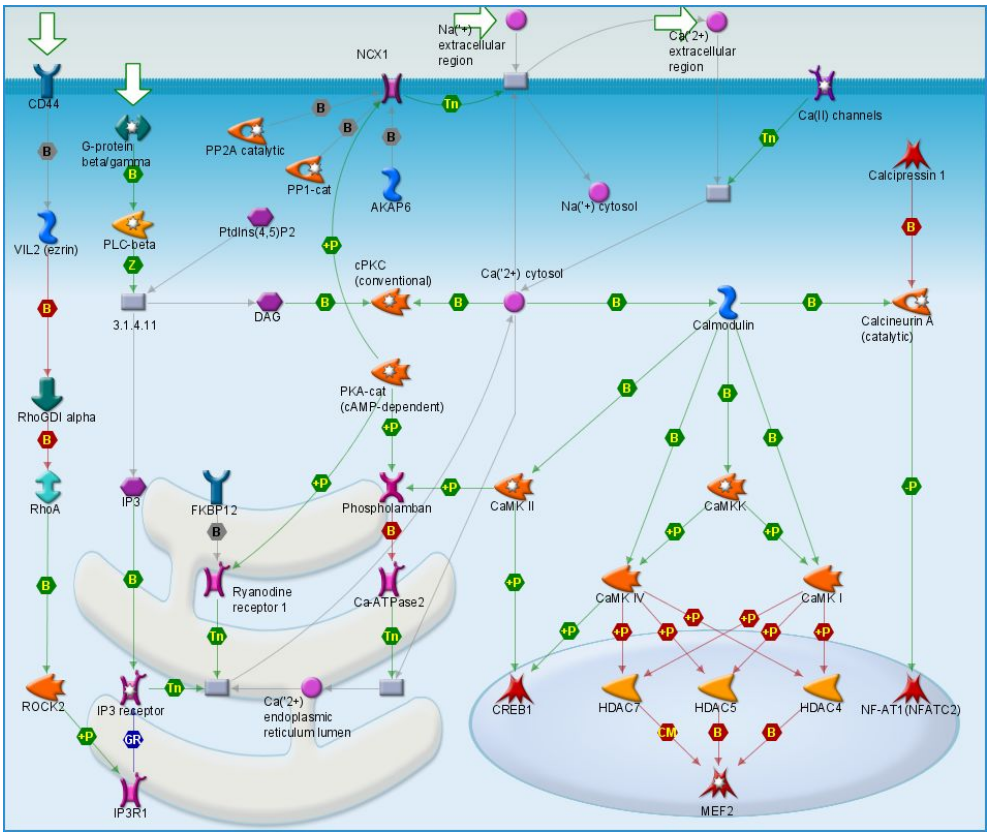

Figure 1.21 Intracellular calcium pathways [31]

1.2 Bone regeneration using electrical stimulation

1.2.1 Bone regeneration process by electrical stimulation

In early 1950s, bone piezoelectricity was reported by Fukada and Yasuda [35]. Endogenous electric field is generated by bone piezoelectricity according to bone contraction or tension. And accompanying the existence of electric field bone formation or bone resorbsion occurs [36]. Based this phenomena, enhancing bone

healing by generating electric field to bone using electrical stimulation device became a basic idea of bone regeneration [37]. As mentioned in former section, electrical stimulation regulates cellular process through modulation of membrane potential. Bone cells also undergo a change of membrane potential by endogenous electric field or electric stimulation. The membrane potential change elicits regulation of cellular process related with electricity. Figure 1.22 demonstrates activation of cellular process pathway through electrical stimulation. Moreover the membrane potential modulated by electrical stimulation activates a voltage-gated calcium channel, makes increase of intracellular calcium concentration. Increased calcium ion activates calcium/calmodulin pathway, then gene transcription in cell is modulated by calcium/calmodulin. Through this cascade event, many cellular processes occur. The regulated processes include increase expressions of BMP-2, BMP-4, TGF-beta1, ALP and VEGF, strong formation of extra cellular matrix, arise of proliferation and differentiation of osteoblast cell, prohibiting bone function failure, encourage of acceleration of bone formation [38-40]. Also the increase of intra cellular calcium concentration affects bone formation through mineralization of bone cell followed calcium phosphate deposition to extracellular collagen fiber [41].

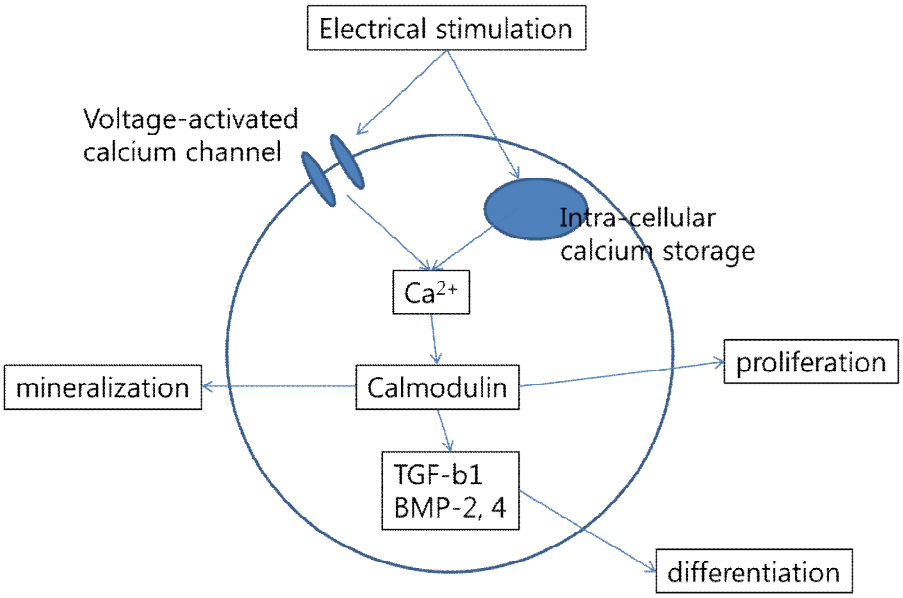

Figure 1.22 Cellular pathways and cellular process regulated by electrical stimulation in osteoblast

1.2.2 Clinical studies of bone regeneration using direct current stimulation

There are two methods for deliver electrical stimulation to bone defect site. One is direct electrical stimulation and another is indirect electrical stimulation. In the method of direct stimulation, an electrode is placed to defect site. In the method of indirect stimulation, an electrode is not inserted into defect site. Instead of insertion of electrode, indirect stimulation method utilizes electromagnetic field which is generated a pair of electrode at the outside of skin. Using direct current stimulation method, concentrated electrical stimulation to the defect site is possible.

This allows an effective stimulation with a small dose of electricity. Also acceleration of bone healing is feasible because cellular process modulation through electrical stimulation can be limited in the defect site. However the method of direct electrical stimulation, insertion of electrodes is inevitable. A surgery for insertion of electrode is necessary. Also there is a risk of infection or inflammation. In case of indirect electrical stimulation method, a relatively convenient administration of electrical stimulation is possible without surgery. But to deliver electrical stimulation, an external stimulator is required and this can disturb a compliance of patients. Also an effect of bone regeneration is hard to concentrate into defect site because other tissue is under the electrical stimulation not only the defect site. In this study, we would like to concentrate the method of direct current stimulation.

Because an electrical stimulation has a good osteoinductive property, there were many clinical trials to achieve rapid healing of bone fracture using electrical stimulation. In 1971 Friedenburg inserted a stainless steel wire into defect site with delivery of 10 μA electrical stimulation to treat nonunion of the medial malleolus and reported the electrical stimulation was effective for the healing of nonunion [42]. This is the first clinical study that administrated direct electrical stimulation to the defect site and reported bone regeneration. After in 1974 Dwyer used electrical stimulation to healing of spinal fusion and reported bone formation [43]. In 1975 Brighton reported the healing of long bone nonunion [44] and in 1977 Torben reported enhancement of bone formation in case of

tibial nonunion using electrical stimulation [45]. In 1977 Lavine used an electrical stimulation to congenital pseudoarthrosis and commented that a combination treatment of bone graft and electrical stimulation would promote bone regeneration [46]. From these early clinical trials the direct current stimulation method is utilized in treatment of spinal fusion, bone fracture, long bone nonunion, congenital pseudoarthrosis and avascular necrosis [47-50]. Although there are some reports that electrical stimulation was not effective to treat bone defect, but many researchers reported that electrical stimulation promote bone healing. Also Brighton tried to find proper electrical stimulation dose through animal and clinical studies and suggested the 20 μA of electrical stimulation is effective to promote bone regeneration [51]. Steinberg suggested a necessary of detailed prediagnosis for bone healing using electrical stimulation [52]. The acceleration of bone regeneration and promotion of bone healing through electrical stimulation is varying according to age of patients, shape of bone defect, parameters of stimulation. However electrical stimulation is considered as a highly osteoinductive tool and related studies are reported continuously.

1.2.3 Development progress of direct current stimulator for bone regeneration

An early device for direct current stimulation to the bone defect

consisted of a power supply and wire or rod shaped electrode which was connected to the power supply. Figure 1.23 shows an early device that was used in the animal study of rabbit tibial nonunion healing in 1970s [53].

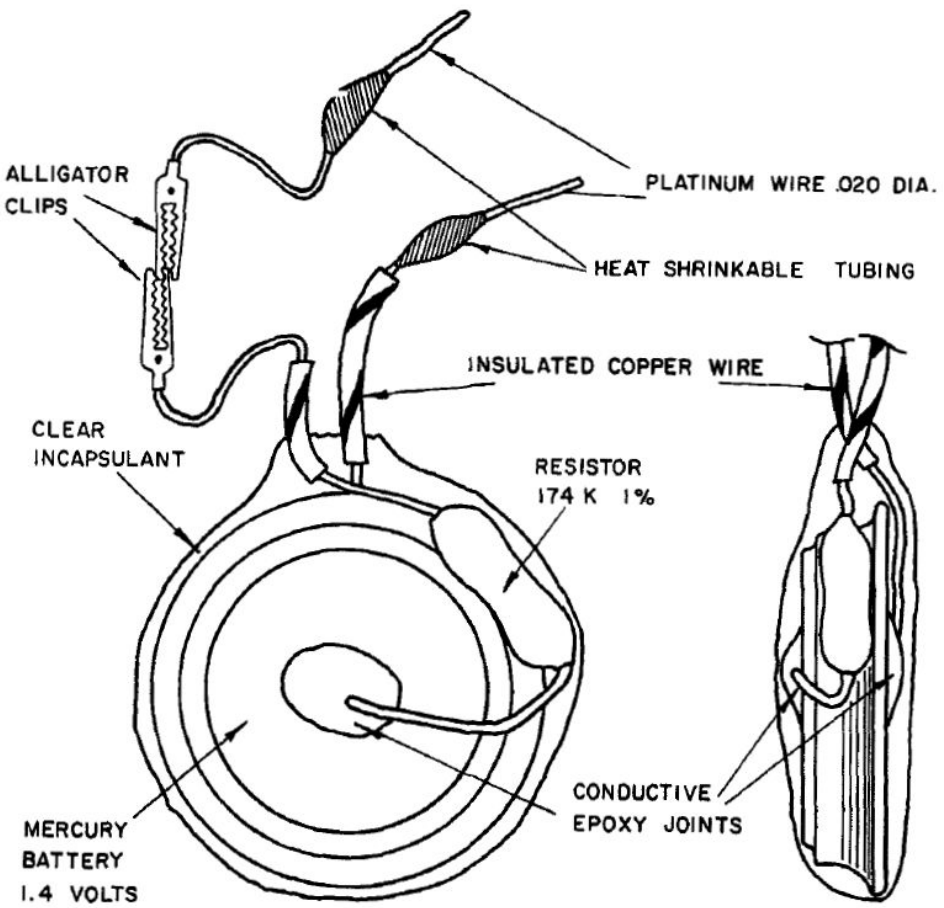

Figure 1. Diagram of experimental unit.

Figure 1.23 An early direct current stimulator for bone regeneration

There are three kinds of major limitations which can be observed from the early electrical stimulation. First is a percutaneous electrode. These electrodes were inserted into the defect site for

treatment. And there was a risk of infection due to exposure of electrode or electrode connection line through a skin. Second is a difficult control of electrical stimulation parameters. The electrodes were connected to battery directly. According to electrode status, a control of delivered current was difficult. Also the early device used a constant DC. If constant DC is delivered continuously, Faradaic products due to charge accumulation produced. These products change local pH and it may cause cell damage. And constant DC accumulates protein to charged electrode. The protein accumulation changes an electrode property, so maintenance of effective electrical stimulation parameter is difficult. Third, a limitation of an effective area comes from electrode shape. The effective area of a wire or a rod shaped electrode is known as 5~8 mm of the electrode surrounding [54]. This means that only a defect area which is located in a certain distance from the electrode receives regeneration effect from electrical stimulation. So if the defect area is formed beyond the effective stimulation area of electrode, bone regeneration effect is limited. It is necessary that an usage of electrode that adjust to the shape of the defect area for concentrated treatment of electrical stimulation.

The early stage of electrical devices for bone regeneration which has limitations as mentioned above were improved gradually, nowadays there are various devices developed and commercialized. Table 1.4 lists up bone regeneration devices using electrical stimulation approved from FDA, these devices is utilized to treatment various bone defects including non-union fracture, spinal

fusion and osteoporosis.

Table 1.4 FDA approved conventional bone regeneration devices using electrical stimulation [37]

Company	Device	Stimulation strategy	Application
Orthofix	Physio-Stim Lite	PEMF	Nonunions for short and long bones
Orthofix	Cervical and Spinal-Stim	PEMF	Spinal fusion
Biomet	OrthoPak 2	CC	Nonunion fracture
Biomet	SpinalPak	CC	Spinal fusion
Biomet	EBI bone healing system	PEMF	Nonunion fracture
Biomet	OsteoGen	DC	Nonunion
Biomet	SpF implantable spine fusion stimulator	DC	Spinal fusion

The improved features of three major limitations of the early devices are as in the following. First, a design of electrical stimulation device which had a percutaneous wire or rod was changed into an implantable device. The first implantable device was used by Paterson in 1984 for treatment of congenital pseudarthrosis of tibia [55]. The implantable stimulation device does not make any exposed electrode or connection line so risk of infection due to percutaneous electrode can be removed. Also the implantable device has minimal postoperative discomfort. For implantation the device was miniaturized and had hermeticity. The device power was supplied by battery so the device size depends on battery size. Also a stimulation period is limited. Second, the device generated electrical stimulation by programmable current generation chip. Using a current source uniform current stimulation was possible regardless of electrode status. Also to avoid issues

from constant DC stimulation, biphasic electrical current (BEC) is using. BEC can avoid charge accumulation and has an effective for bone formation and growth factor recruiting. Third, a wavy wire or mesh electrode was developed to apply in various shapes of bone defect. These electrodes can transform its geometrical shape so that closer and wider contact to defect site is achievable. OsteoGen device of Biomet in figure 1.24 has improvements mentioned above [56]. In this device a current stimulator is packaged with titanium and silicone rubber. Implantable period is 6 months and during the period the device is powered by battery imbedded in titanium package. This device uses a pair or many pairs of titanium wavy electrode for electrical stimulation. By a wavy electrode the contact area between the electrode and defect site increases. This device can be applied for treatment of bone defect such as nonunion fracture, and fixation of bone grafts. Although this device improved some limitations of the early device, there are other limitations. First, this device used its titanium package as anode. In this case electrical stimulation is not restricted in the area of bone defect, so the effect of electrical stimulation is distributed to other tissue. Second, although wavy or mesh electrode has an advantage to treat bone fracture or nonunion, it is not proper to bone grafting or spinal fusion which need three dimensional delivery of electrical stimulation. Third, after bone healing, the package should be subtracted so two surgical procedure is necessary. Fourth, after implantation, change of stimulation parameter is impassible. Fifth, the stimulation period is restricted by battery life.

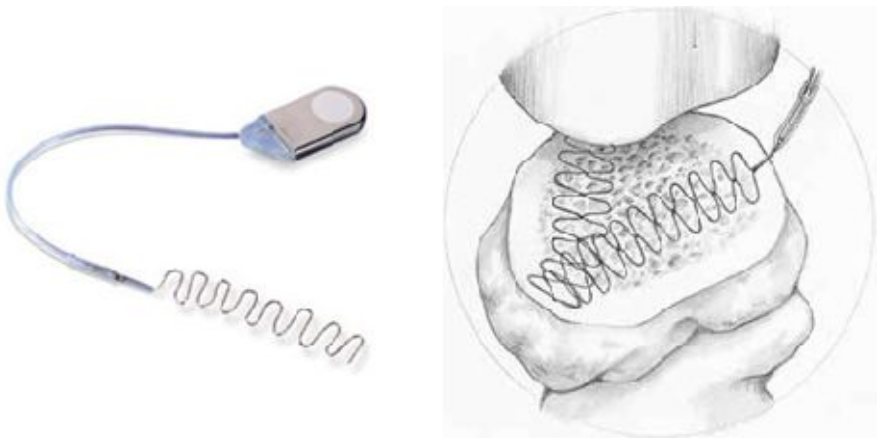

Figure 1.24 Bone regeneration device of Biomet and schematic of application of the device to bone fracture

1.3 Bone regeneration therapy

1.3.1 Existing bone regeneration therapies

Although bone tissue is capable of self-regeneration, if defect site is over critical size, it is difficult to regenerate by oneself. Also it takes long period to heal and even though after recovery, it is possible to acquire bone structural disorder such as non-union. Therefore a proper therapy is necessary to make rapid healing of bone defect. For the existing bone regeneration therapies to treat bone defect, block grafting, distraction osteogenesis and bone splitting are executed [57]. Block grafting is a surgical procedure that transplants a bone graft to bone defect site. Autograft is the most preferred because the graft is harvested from the patient's

own body so there is less risk of infection or immune reaction compare with other graft [58]. Grafts are harvested from intra, extra oral, iliac creat, finula, mandible and skull usually. However to harvest autograft, additional surgery should be conducted from the patient who already have bone fracture. Also the volume of harvest is limited. Distraction osteogenesis (DO) is a surgical procedure that utilizes a self-repair character of bone. This is used in reconstruction of skeletal deformities or bone increase [59]. In this procedure, a target bone is split into two pieces using corticotomy, and the end of divided bones is drawn gradually. Then a gap generated between the bones is filled with new bone by self-repair of bone. Through this process the construction and bone healing occurs. The period of pulling a bone is called to be a distraction phase. Then if a sufficient increase and reconstruction of bone is achieved, consolidation period follows. This procedure takes an advantage that surround soft tissue grows simultaneously with bone grow. But a possible procedure region is limited and it is hard to conduct in case of a large bone defect. In bone splitting, a bone is split using a rotating instrument or ultrasonic device. After bone spitting, distraction of bone using osteotome follows. Then an implant is inserted to split bone and filled with autologous bone or replacement material. This procedure is difficult to conduct if a width of bone to be split is narrow [60].

1.3.2 Bone regeneration therapy using stem cell graft

In case of more than 1 cm of bone defect, bone regeneration relies on bone graft transplantation such as block grafting [61]. In addition of bone graft transplantation using autograft, allograft or xenograft, a bone regeneration therapy using stem cell graft is introduced with development of tissue engineering, and the stem cell grafting is conducted successfully. The bone regeneration therapy using stem cell graft utilizes a method of tissue engineering in bone repair. A graft seeded stem cells is implanted into bone defect area and the stem cell in graft is ossificated into bone tissue. As important components in stem cell grafting, there are osteoblast cell will be differentiated to bone cell and morphological signals that makes stem cell differentiation [62]. For the cell used in stem cell grafting, autologous cell is considered as a golden rule. But there are some restriction that their limited available cell amount and additional surgery for harvesting. Therefore the usage of stem cell is increased for bone graft because stem cell has a pluripotency and a large amount of stem cell can be harvested by cell culture. After harvest from donor, the stem cells are cultivated at *in vitro* circumstance by incubator. After the cells are proliferated sufficiently, they are inoculated to a biodegradable material which has a porous structure such as collagen sponge or hydrogel for cell adhesion. Finally the cell graft is transplanted into bone defect site. The stem cell graft should be set into a proper structure to be

protected from external damage and to be fixed in defect site. The structure that acts containment system for stem cell graft is made by biodegradable material or titanium mesh that has a high osteointegrity [63]. Morphological signals applied to stem cell to make differentiate into bone cell are important in bone graft transplantation procedure. As the signals that induce bone differentiation, mechanical stimulation like repetition of shear stress, ultrasonic, heat and infrared light are known [64]. Also bone differentiation is mediated by injection or activation of bone morphogenetic protein (BMP) −2, 4, 7 or transforming growth factor beta (TGF−β) [65]. It is necessary for a successful application of bone graft transplantation that a proper apply of two important factors, osteoblast cell and morphogenetic signals.

Especially in the case of osteoblast cell, the expansion of cell numbers by *in vitro* cell culturing is required. For cell expansion, more than a month of long period is required. Consequently there are disadvantages of high cost, infection risk, and low cell viability due to the cell culture procedure [66]. Therefore for apply the stem cell graft transplantation procedure and successful bone regeneration, it is important that harvesting more viable cell and more amount of cell [66].

1.4 LCP as bone substitute

Liquid crystal polymer (LCP) is a kind of aromatic polyester. It has

very low water absorption rate, inert chemical reaction property, excellent mechanical property, and biocompatibility [67]. Figure 1.25 shows the crystal unit structure of LCP. A solid monomer and soft monomer is arranged as consistence in aqueous status.

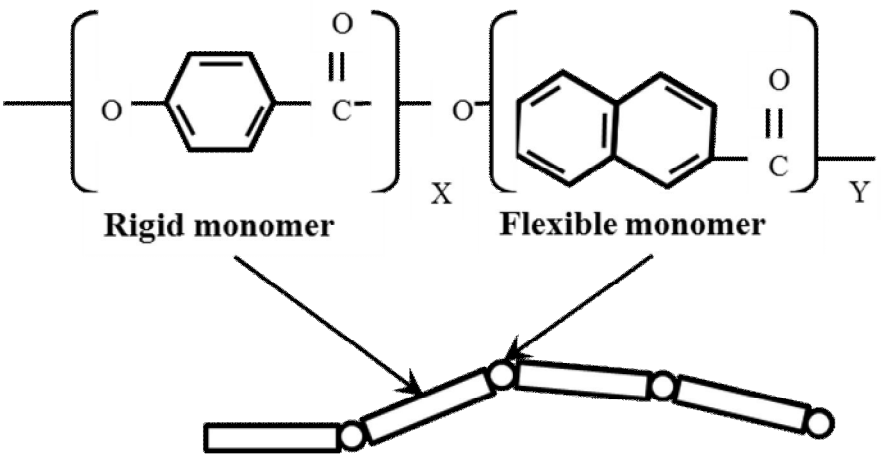

Figure 1.25 Crystal unit structure of LCP

LCP is thermoplastic polymer. It can be deformed into various shapes in high temperature. Also LCP can be adjust in semi-conductor process. A film type LCP can be made in multi-layer structure. From these characteristics of LCP, active studies of LCP as a package material for neural prosthetic device and a substrate material of electrode [68-70]. Furthermore LCP is a material that has a high osteointegrity, it is studied as bone substitute material [71].

Kettunen et al. designed LCP in shape of a rod and drilled a femur of rabbit and dog. Then they inserted the LCP rod to bone defect and examined bone adhesion and implant failure after 1 year of

follow up for rabbit and 4 years of follow up for dog. After examination, they obtained a sufficient stability in fixation. There were no evidence of tissue reaction and no sign of implant failure both of rabbit and dog [71-72].

1.5 Objectives of the dissertation

As an excellent osteoinductive signal, electrical stimulation has a positive effect on bone regeneration. The conventional bone regeneration devices using electrical stimulation is used for bone repair and regeneration. However the conventional device is not proper to apply in bone graft transplantation for the case of large bone defect. It is necessary for application of bone grafting using electrical stimulation that electrical stimulation should be delivered the entire of bone graft that has three-dimensional area effectively. The electrode of the conventional device is wire shape and the electrical stimulation is delivered to around of the wire electrode only so it cannot deliver electrical stimulation to three-dimensional bone graft. To apply electrical stimulation into bone grafting, the shape of electrode is a structure can contain the bone graft for delivering electrical stimulation to entire of the bone graft. In this dissertation, development of bone regeneration device that accelerate bone formation by stimulating electric current pulses which have high osteoinductive property for bone graft transplantation procedure that conducted in the case of large bone

defect is demonstrated. Also the evaluation of bone regeneration using the device is reported. To achieve these objects it is required several steps. First is a development of a device that can deliver electrical stimulation to stem cell graft at *in vivo* circumstance. Using the device cell proliferation and up-regulation of cell viability will be reported. For the next step, a development of bone regeneration device using electrical stimulation for targeting a rabbit mandibular defect model by improvement of cell culture device developed before. Using this device, tissue engineered bone regeneration with combined treatment of electrical stimulation and growth factor will be conducted. For the last, by improving former device, LCP-based bone regeneration device will be designed. Through this device, the concept of fully implantable, battery-less, chronic bone regeneration device which acts bone substitute will be introduced.

Chapter 2 Materials and Methods

2.1 Implantable bioreactor device

2.1.1 Device configuration

Implantable bioreactor device consists of three components. First is a bioreactor chamber. A stem cell graft which is cultivated intracorporeally and electrode which delivers electrical stimulation to the cell graft are set into the bioreactor chamber. The bioreactor should be made with a biocompatible material because it will be implanted in the body. Also the chamber should have proper shape and size for relevant to the experimental animal. And the chamber should be designed as the chamber allows interaction of body fluid into the inside of the chamber. The designed chamber is shown in figure 2.1.

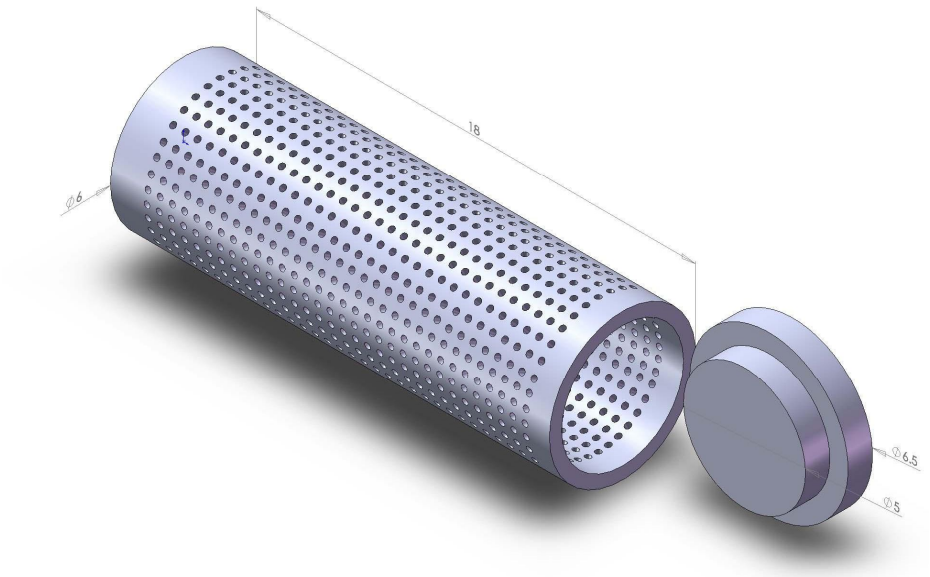

Figure 2.1 Design of the bioreactor chamber

We designed the chamber in the form of a cylinder using Teflon which has a biocompatibility. The length of the chamber is 15~17 mm according to electrode type. The size of the holes was 300 μm in diameter along the surface of the wall of the chamber to allow interaction of body fluid and nutrition into the inside of the chamber. The second component of the bioreactor device is a current generator chip. This stimulation chip was produced by Intergration circuit design education center (IDEC) 80th Samsung 0.18 μm process and the circuit configuration is same as our previous stimulation chip [73 Electrical stimulation type produced by stimulation chip is charge-balanced biphasic electric current pulse. The parameters of BEC can be selected the amplitude from 2 μA to 300 μA in 2-μA steps, the duration and the frequency from 16 μs to 512 μs in 16-μs steps and from 32 Hz to 1 kHz in 32-Hz steps

respectively by attaching external components on the chip PCB.

This chip is bonded to PCB which has 16 mm diameter by wire bonding. Then epoxy is covered the chip to protect from external shock. The stimulation parameter setting is conducted by external component assembled together and switch selection is executed by soldering. Figure 2.2 shows the feature of the bonded stimulation chip on the PCB with external components.

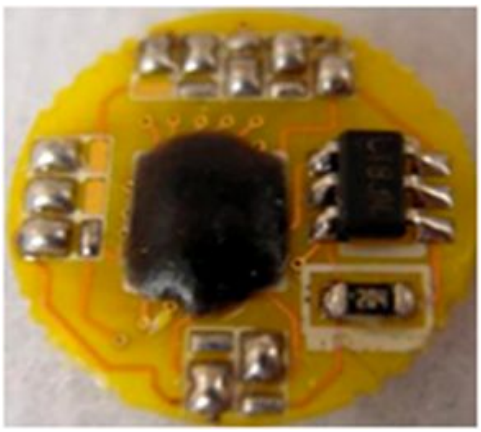

Figure 2.2 Feature of the stimulation chip bonded on the PCB

The current generator chip assembled on the PCB is supplied a power by a button style battery which is connected through wire. The battery for power supply can be selected in various types according to parameters of the electrical stimulation. Also the entire device is implanted in a body so the current generator chip should be hermetic packaged to prevent a failure of the device. In this study, silicone elastomer (NUSIL, MED-6215) is used as a package material. The package process is conducted with package molds which are made by acryl. Figure 2.3 shows three types of

acryl molds used in silicone elastomer packaging.

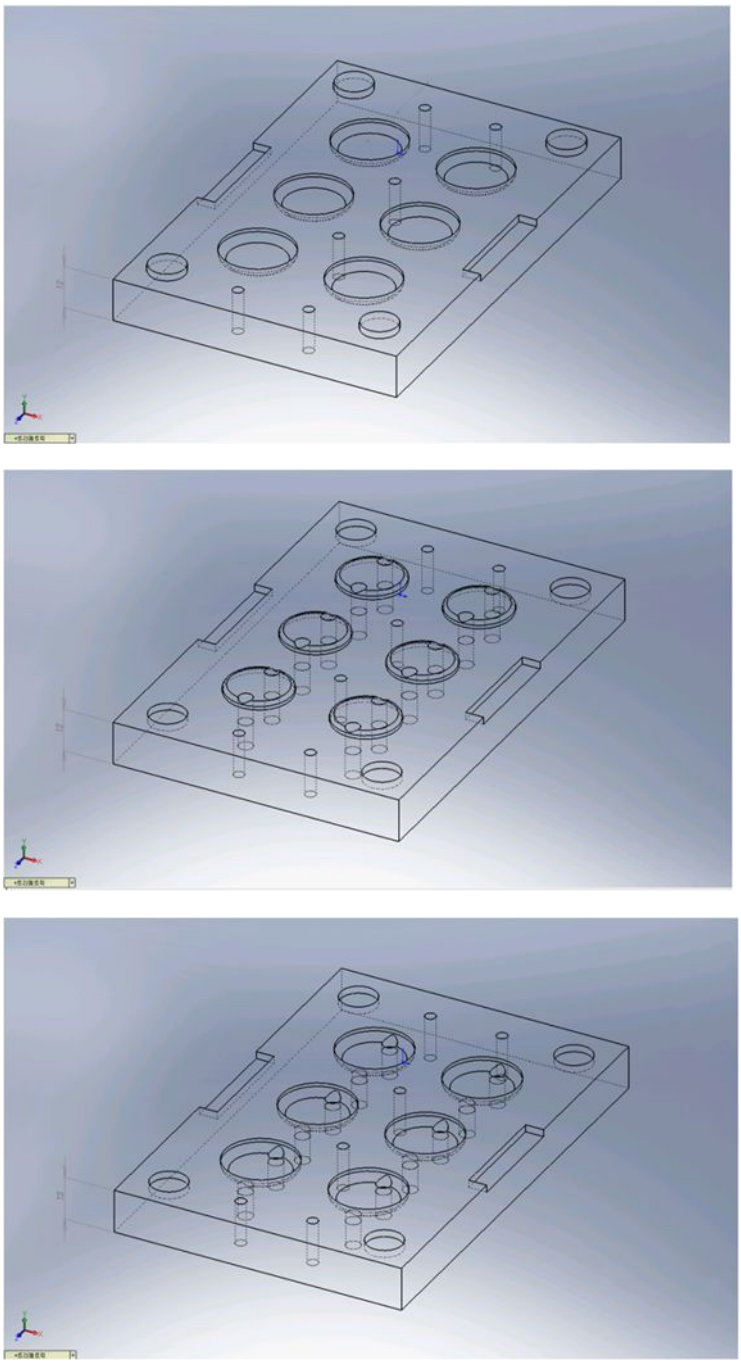

Figure 2.3 Three types of packaging molds used in current generator device. (A) is mold A, (B) is mold B, (C) is mold C

Using the packaging molds, production of six packages of current generator chip is possible at once. The size of the sealing package differs according to type of battery. The process of packaging follows. First, adequate amount of silicone elastomer and hardening agent is taken in a ratio 10:1 respectively. They are mixed well then air is removed from the mixture using a centrifuge. After that, the mixture is taken by 3 ml through a disposable syringe. Then additional air removal using vacuum chamber is conducted. By these processes, it can be achieved that elimination of vacancy due to bubbles in the finally sealed package. The vacancy from bubbles makes main passages for infiltration of body fluid into the stimulation chip. So the vacancy is the cause that makes device failure, the air removal process is necessary for packaging with silicone elastomer. After air removal, mold A is covered with mold B and they are fixed with bolts. Then mixture of silicone elastomer is casted in the molds through the disposable syringe containing the mixture. After that a curing process is conducted for 30 min in the temperature of 90 degree. After curing, mold B is separated from mold A. Through this process the elastomer is made in a shape of dish. Then the current generator chip which is connected to electrode and battery is put on the elastomer dish, and mold C covers mold A and fixed with bolts. Then second silicone elastomer casting in the molds through the disposable syringe containing the mixture is conducted. Then curing step follows. Because a battery is cured together, the curing temperature should not be over to 45

degree. After 10 hours of curing, the packaged current generator chip is separated from mold. The packaged device has a shape of thick coin which diameter is 20 mm and thickness is 4 mm in case of using 1620 battery. The package can protect a device failure due to infiltration of body fluid for a month of an implantation period. In figure 2.4, the packaged current stimulation ship and battery with silicone elastomer is shown.

Figure 2.4 A feature of the packaged PCB with silicone elastomer

The last component of bioreactor is an electrode which delivers electrical stimulation to the stem cell graft inside of the bioreactor chamber. The package volume of the current stimulation chip is as large as the bioreactor chamber, so if the chamber and chip package are implanted into same area together, it may cause hindrance of animal movement and pain due to large volume of implant body. This can cause an unexpected effect to the results. So the electrode should have a sufficient length of connection line to allow the current stimulation chip and the bioreactor chamber is implanted

with making an adequate distance. This connection line should have a flexibility and biocompatibility. Also it should have to achieve convenience for surgery and to eliminate hindrance of animal movement. Combining three components, it is possible to make an implantable bioreactor device. And using this device, intracorporeal cell culture is possible through setting cell graft into the chamber at *in vivo* circumstance.

2.1.2 Bioreactor using titanium electrode

Figure 2.5 is a schematic of a bioreactor that uses titanium electrode.

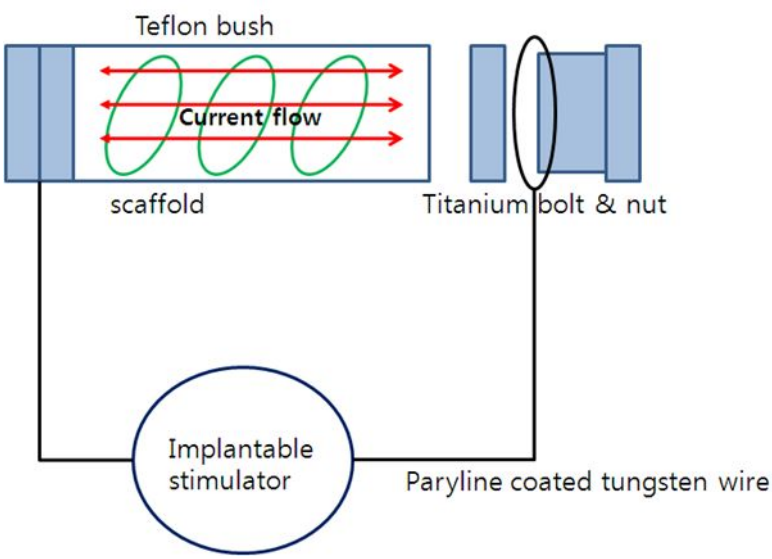

Figure 2.5 A schematic of bioreactor that uses titanium electrode

Titanium electrode consists of a pair of volt and nut which were

made by titanium. The head of the volt is circular shape and outer diameter of volt is 8 mm and inner diameter is 6 mm. The length of volt head is 1 mm, the entire length of volt is 4 mm. The shape of nut is circle and its outer diameter is 8 mm and its inner diameter is 6 mm. This electrode pair is connected to PCB of current generator chip through a tungsten wire which has a diameter of 100 μm and a length of 100 mm. The tungsten wire is fixed in joint of the volt and nut. For titanium electrode, the bioreactor chamber was designed in a form of cylinder which has a length of 15mm, diameter of 8mm using Teflon. The chamber was designed as a hollow cylinder and titanium electrodes were inserted into the both end of the chamber. In the case of titanium electrode, a current path is generated in the direction of the longitudinal direction of the chamber. Figure 2.6 shows a designed bioreactor chamber and titanium electrode and figure 2.7 demonstrated the entire feature of bioreactor system with titanium electrode.

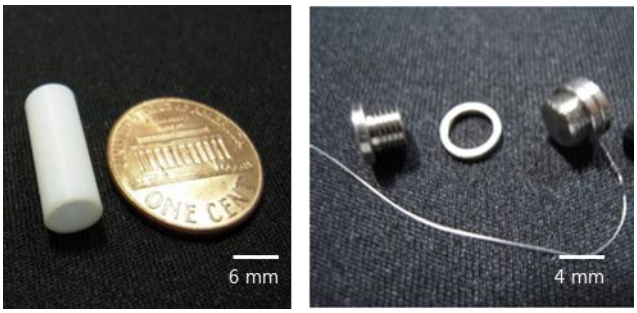

Figure 2.6 Bioreactor chamber and titanium electrode

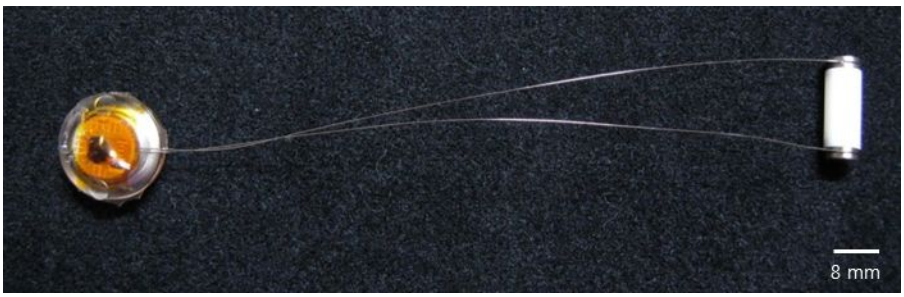

Figure 2.7 The entire feature of bioreactor using titanium electrode

2.1.3 Bioreactor using polyimide electrode

Figure 2.8 is a schematic of the bioreactor using a polyimide electrode.

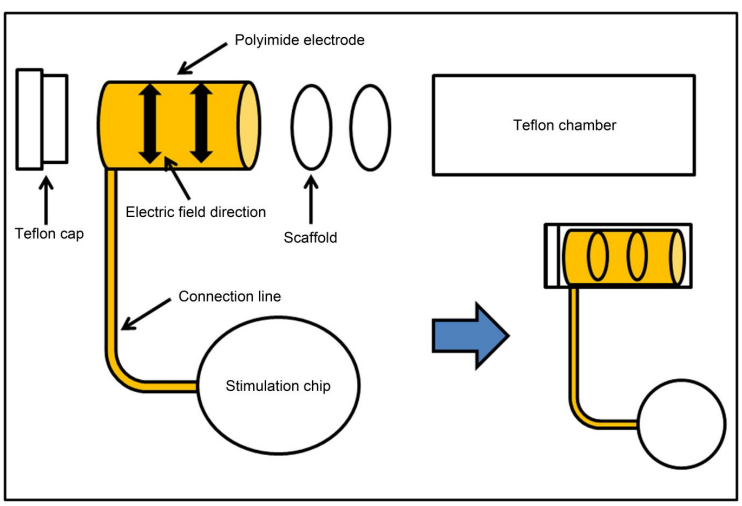

Figure 2.8 A schematic of the bioreactor using a polyimide electrode

Electrode was designed using biocompatible, flexible polyimide. Polyimide has been generally used as an electrode substrate material of various neural prosthesis devices [63]. The electrode

part and connection line of the polyimide electrode were made by polyimide also, and the electrode site and conductor of connection line was gold. Figure 2.9 shows the electrode part of polyimide electrode.

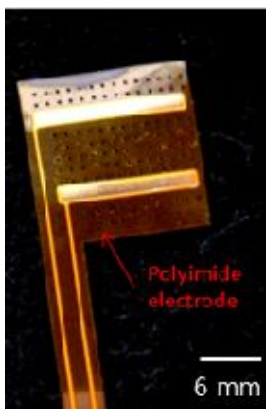

Figure 2.9 Electrode part of the polyimide electrode

This electrode part put into the bioreactor was a 15 mm square shape, and had two rectangular shaped gold patterns of which length was 12 mm and width was 3 mm. And except the area of gold patterns, electrode area was evenly holed sizing 300 μm in a diameter. The two gold patterns were placed face to face when the electrode was rolled up cylindrically to put it into the bioreactor chamber.

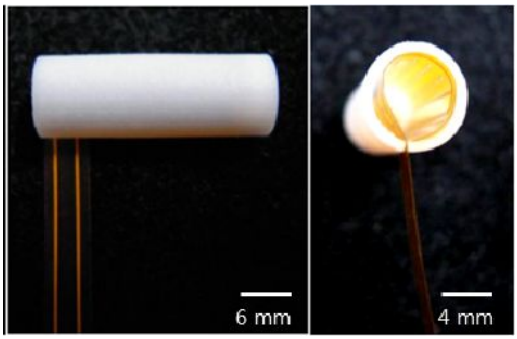

Figure 2.10 The setting of polyimide electrode into the bioreactor chamber

Total length of the connection line of the polyimide electrode was 100 mm and the width was 5 mm. This connection line was connected to PCB of current stimulator chip. Chamber, where the electrode is inserted into, was designed in a form of cylinder which has a length of 17mm, diameter of 8mm using Teflon. It is designed as one side blocked cylinder and has a Teflon cap to block other side after put into the stimulation electrode and scaffold. In the case of polyimide electrode a current path is generated in the direction of the center of the chamber. Figure 2.11 shows the bioreactors which uses polyimide electrode.

Figure 2.11 The entire feature of bioreactor using polyimide electrode

2.1.4 *In vivo* cell proliferation experiment

The process of *in vivo* cell proliferation experiment follows. First stem cell was inoculated on collagen sponge. Then the collagen sponge was set into bioreactor device and the bioreactor which contains stem cell graft was implanted into a rat. After 2 weeks of surgery, the cell graft was harvested and the cell proliferation and cell viability were evaluated.

2.1.4.1 Preparation of collagen sponge

Type I atelocollagen powder (Bioland, Korea) was dissolved in 0.001 N HCl at a concentration of 20 mg/ml, and CS (Sigma Chemical Company, St. Louis, MO) was dissolved at a concentration of 2 mg/ml. The collagen-CS solution was poured into a 60 mm dish and was lyophilized by freeze-drying (Samwon Freezing Engineering Co., Korea) at -80° C for 48 h. The collagen sponge was incubated in 20 ml of 40% (v/v) ethanol containing 50 mM 2-morpholineoethane sulfonic acid (MES, Fluka Chemic AG) (pH 5.5) for 30 min at room temperature. The collagen sponge was immersed in 20 ml of 40% (v/v) ethanol containing 50 mM MES (pH 5.5), 24 mM 1-ethyl-3-(3-dimethyl aminopropyl)carbodiimide

(Fluka Chemic AG), and 5 mM N-hydroxysuccinimide (Fluka Chemic AG) for 12 h at room temperature. Once the reaction was complete, the collagen sponge was washed twice in 0.1 M Na2HPO4 (pH 9.0) for 12 h. The scaffolds were then washed twice in 1M NaCl for 6 h, then in 2 M NaCl for two days. Finally, the sponges were rinsed with distilled water. The collagen sponges were lyophilized by freeze-drying and were cut by the shape of circle that has a diameter of 5 mm and a thickness of 1 mm and then sterilized with γ-irradiation at 15 KGy. The collagen sponge has average ultimate tensile strength of 1.5-0.05 MPa, and compressive moduli of 1.80 ~ 17.29 kPa with a loose network of collagen fibrils and an approximate pore size of 80~150 μm.

2.1.4.2 Preparation of hMSCs

The commercial hMSCs (Lonza, Walkersville, MD) derived from bone marrow were cultured in a specific culture medium provided from the maintenance company under a humidified atmosphere of 5% CO_2 at 37° C. The hMSCs were inoculated onto a collagen sponge. After approximately 3-h of incubation, high-glucose Dulbecco's modified Eagle's medium supplemented with 10% heat-inactivated fetal bovine serum was added to the cells. The next day, cells seeded on a collagen sponge were placed inside the bioreactor and exposed to an electric field formed by the flow of current from the bioreactor.

2.1.4.3 Process of animal experiment

Every *in vivo* experiment was performed in accordance with the "Recommendations for Handling Regulation for Laboratory Animals for Biomedical Research" compiled by the Committee on the Safety and Ethical Handling Regulation for Laboratory Experiments in the School of Dentistry at Seoul National University. Male SD rats (6 week, n=4) were used in every *in vivo* experiments. After anesthesia, the both side of the thigh of the animal was incised, the bioreactor chamber that contains stem cell graft was placed in the upper thigh. And the package of stimulator was placed in the lower thigh. The animal was then sutured. The single type of electrode was used in one animal, and each animal has two bioreactor chambers in the body but electrical stimulation was delivered in only one bioreactor chamber. Electrical stimulation was delivered in the form of charge-balanced biphasic current pulses at an amplitude of 20 μA, a duration of 100 μs, and a frequency of 100 Hz. After the surgery, electrical stimulation was performed for 1 week. And the cell culture period was 2 weeks. After cell culture period, the animal was sacrificed, the bioreactor and collagen sponge were extracted, and a quantitative evaluation of cell proliferation was conducted using a MTT assay. Figure 2.12 shows entire process of the surgery.

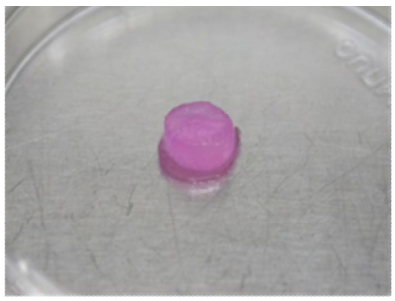

Cell scaffold preparation
Collagen sponge + hMSCs

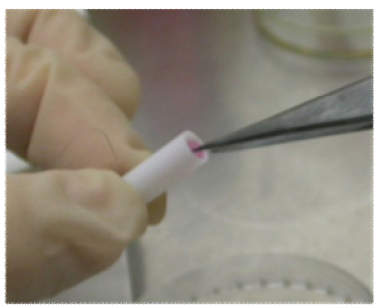

Scaffolds setting

Implantation for 4 weeks

Figure 2.12 The process of cell proliferation experiment using bioreactor

2.1.5 Assessment of cell proliferation

2.1.5.1 MTT assay

The proliferation of cells cultured on a collagen sponge *in vitro* or *in vivo* was assessed at 2 or 4 days using a the Cell Counting Kit-8 (Dojindo Laboratories), which employs tetrazolium salt, WST-8 [2-(2-methoxy-4-nitrophenyl)-3-(4-nitrophenyl)-5-(2,4-disulfophenyl)-2H-tetrazolium, monosodium salt]. Processes were carried out according to the manufacturer's protocol. The amount of yellow-colored product was measured at a wavelength of 450 nm using a microplate reader and was directly proportional to the number of viable cells in the culture media. The optical density (OD) values of samples represent the index of cell proliferation. This assay was repeated for three or four independent samples (n = 3-4).

2.1.5.2 Scanning electron microscopy (SEM)

The sponges were washed twice with PBS. Cells adhering to the sponges were fixed with 2.5% glutaraldehyde. After washing thrice with PBS, the adhered cells were dehydrated in an ethanol-graded series and allowed to dry on a clean bench at room temperature. The sponges were then coated via the Au-Pd sputtering method. SEM observations were conducted with a Hitachi s-4700 field

emission SEM at 30 kV.

2.1.5.3 Reverse transcription=polymerase chain reaction (RT-PCR)

The collagen sponge with hMSCs was washed with PBS solution and chopped into small pieces. After adding 0.5 mL of TRIzol reagent (Invitrogen, Life Technologies) directly to the chopped sponge, the total RNA was extracted and then subsequently treated as prescribed in the manufacturer's instructions. The total RNA was extracted by adding 0.5 mL of TRIzol reagent (Invitrogen, Life Technologies) directly to the chopped sponge. One microgram of RNA from each sample was subjected to cDNA synthesis using SuperScriptTM Reverse Transcriptase II (Invitrogen) and oligo (dT)12-18 primer (Invitrogen) in a 20 mL reaction volume according to the manufacturer's instructions, and RNA complementary to the cDNA was removed using E. coli RNase H (Invitrogen). One microliter of cDNA was then subjected to a polymerase chain reaction using the following amplification profile: predenaturation at 94 C for 40 s, amplification (denaturation at 94° C for 40 s; annealing at 60° C for 40 s; an extension at 72° C for 1 min) for 30 cycles, followed by a final extension step at 72° C for 10 min. PCR was performed in a DNA thermal cycler (model PTC-200; MJ Research, Inc.). Ten microliters of each of the PCR product were electrophoresed on 1.5 % agarose gel in the presence of ethidium bromide, and the bands were visualized using a Gel

Documentation System (Vilber Lourmat). The human primer sequences were as follows: type I collagen (GenBank# BC036531) forward, CGA AGA CAT CCC ACC AAT CAC; reverse, CAG ATC ACG TCA TCG CAC AAC; β-actin (GenBank# BC004251): forward, ATT GCC GAC AGG ATG CAG AAG; and reverse, TTG CTG ATC CAC ATC TGC TGG.

2.2 Implantable electrical stimulation device for bone regeneration

2.2.1 Configuration of bone regeneration device

The implantable electrical stimulation device for bone regeneration was designed by improving the implantable bioreactor device developed before. Figure 2.13 demonstrated the designed bone regeneration device.

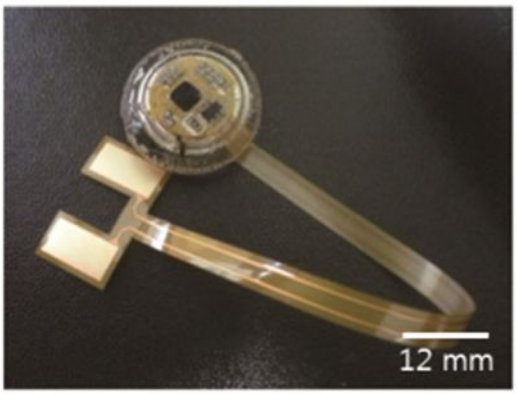

Figure 2.13 The entire feature of bone regeneration device

The bone regeneration device was composed with two components of electrical stimulator and electrode which can contain a stem cell graft. The current generator chip, PCB, and battery used in bone regeneration device were same as in the bioreactor device. Also the package material and method were identical with the case of bioreactor. The flexible polyimide electrode of this device can effectively deliver electrical stimulation to local three-dimensional tissue area by changing the shape of the electrode fitting to the target tissue. Also by applying a containment system made with biodegradable material or high osseointegrative material such as titanium, *in vivo* bioreactor circumstance with electrical stimulation can be set in the body. Therefore stem cell grafting with electrical stimulation is possible by setting the cell graft into bioreactor circumstance which is made by the combination of electrode and containment system. Furthermore through scaffold material or external treatment, injection or secretion of growth factor which helps cell proliferation or differentiation is possible.

2.2.2 Electrode for bone regeneration of rabbit mandible

Using polyimide as the electrode substrate material, we designed an electrode that was feasible for local stimulation of a three dimensional bone scaffold. A pair of gold electrodes 5 mm in width and 10 mm in length was patterned by electroplating onto the

polyimide substrate which was 20 mm in width and 12 mm in length. The pair of gold electrodes was 8 mm apart from each other. After electroplating, a non-patterned section of the polyimide substrate 6 mm in width and 9 mm in length between the pair of gold electrodes was cut off. The two gold electrode sites were placed face to face when the section of the gold electrode site was folded at 90 degrees. The electrode could then be set into the PCL outer box. In the PCL outer box, electrical stimulation was delivered to hBMSCs on a collagen carrier between the two gold electrode sites. Also, the polyimide electrode had a 10 cm polyimide connection line. Through this line, the electrode and stimulation chip were connected and the electrical stimulation was delivered. The connection line allowed the stimulation chip to be implanted onto a part that was distanced from the defect site.

2.2.3 Preparation of collagen sponge

A collagen sponge was prepared from the cross-reaction of type I collagen (Bioland Co.) and chondroitin-6-sulfate (Sigma Chemical Company, St. Louis, MO, USA) as previously described section. The shape of prepared collagen sponge is 13 mm x 6 mm of rectangular shape that has a thickness of 1 mm.

2.2.4 hBMSCs culture

Commercial hBMSCs (Lonza, Walkersville, MD) derived from bone marrow were cultured in a specific culture medium provided by a maintenance company under a humidified atmosphere of 5% CO_2 at 37° C. The hBMSCs were inoculated onto the collagen sponge (1 x 10^5/sponge).

2.2.5 Preparation of hydrogel

Hyaluronic acid (HA) (0.25 mmol, MW 23 kDa, Lifecore, USA) was dissolved in 40 ml of distilled water and 1-Ethyl-3-(3-dimethylaminopropyl)-carbodiimide (EDC, 0.24 g, 1.25 mmol, Sigma-Aldrich, USA), 1-hydroxybenzotriazole hydrate (HOBT, 0.17 g, 1.25 mmol, Fluka, Switzerland) and adipic acid dihydrazide (ADH, 2.2 g, 12.5 mmol) were added to the solution [75]. The EDC-mediated the coupling reaction between the carboxyl group of HA and the hydrazide group of ADH continued, with stirring, at room temperature for 8 h. HA-ADH was dialyzed against 100mM NaCl for 2.5 days and distilled water for 1 day using a dialysis membrane (MWCO 14,000, SpectraPor, USA). N-acryloxysuccinimide (NAS, 0.5 g, 3 mmol, Polyscience, USA) was subsequently added to the HA-ADH solution. The reaction continued, with stirring, at room temperature for 12 h. HA-ADH-NAS was dialyzed extensively against 100mM NaCl for 2.5 days and distilled water for 1 day. The product was then lyophilized for 3 days to obtain solid acrylated HA (HA-Ac). For the preparation of

the gel, MMP-sensitive peptides (GCRDGPQGIWGQDRCG, AnyGen, Korea) were added to the acrylated HA solution [75] with the same molar ratio of acryl and thiol groups. The HA-based hydrogel was formed via a Michael-type addition reaction [75] Cell-adhesion peptides (RGDSP, AnyGen, Korea) were also immobilized on the acrylated HAS with a molar ratio of 20% of the acryl groups of the HA. The reaction mixture, carrier-free rhBMP-2 (5㎍, R & D Systems, USA) and the collagen sponge seeded with the hBMSCs were incubated at 37° C for gelation. These HA-based hydrogels with the collagen sponge were set into the PCL outer box and implanted into the rabbit mandible defect site as bone substitutes.

2.2.6 Preparation of PCL containment system

The outer box as a containment system, which creates a space for the hydrogel, stem cells, and the electrical stimulation device, was positioned at the rabbit mandibular defect. It was composed of four walls: the buccal, lingual, lower and upper walls. The upper wall prevented new bone ingrowth into the bone defect space from residual alveolar bone, and the right and left sides were open, though they were closed by neighboring bone surfaces at the bone defect area (7 x 7 x 15mm), and new bone ingrowth into bone defect space was allowed. The outer box was prepared using polycaprolactone (PCL) (average MW ~42,500, Sigma-Aldrich, St. Louis, MO) which was softened in hot water (60 ℃). It was built by

bonding four plates (8 (W) x 15 (L) x 1 mm (T)) of PCL with a hot spatula. Numerous pores (1 mm in diameter) were formed for blood and nutrition flows through the walls of the PCL plates using a dental fissure bur (Mani, Inc., Japan) before fabricating the box. The PCL outer box was then coated with calcium phosphate crystals to improve cell adhesion using modified methods described in previous reports [76]. After the sterilization of the PCL outer box using gamma irradiation, the electrode of the electrical stimulation device, the hydrogel and the collagen sponge seeded with the hBMSCs were set into the PCL outer boxes. The PCL outer boxes were then implanted into the rabbit mandibular defect sites.

2.2.7 Animal experiment

2.2.7.1 Animal experiment configuration

Male New Zealand white rabbits (n=5, 3~3.5kg) were used. The bone defect is given into intra sub-mandibular area of the rabbit and the complex bone regeneration system which is composed with PCL outer box, collagen sponge with stem cell, hydrogel containing rhBMP-2, and electrode of bone regeneration device is implanted into the defect site. The used electrical stimulation parameter is follows; amplitude of 20 ㎂, duration of 100㎲, frequency of 100 Hz, charge-balanced biphasic current (BEC) pulses, period of 7 days. And the experimental group is divided into three groups

according to existence of electrical stimulation and the application method of rhBMP-2. In Group 1, rhBMP-2 was mixed with hydrogel, and electrical stimulation was not applied although the electrode was set into the PCL outer box. In Group 2, rhBMP-2 was added in same manner as in Group 1, but electrical stimulation was applied. In Group 3, electrical stimulation was applied, and rhBMP-2 was injected to the defect site directly (5㎍/defect) 1 week after the end of the electrical stimulation.

2.2.7.2 Animal experiment process

For anesthesia, Zoletil (20mg/kg) and Rompun (10mg/kg) were used. For the fabrication of the bone defect, a resection (1.5 cm long and 0.7 cm high from the inferior border of the mandible) of the mandibular body was done, where alveolar bone with teeth was preserved with continuity with the residual mandibular bone; because mandibular stabilization with miniplates after the resection of mandibular body including the alveolar bone with teeth would be unstable, the loosening of the miniplate and screws was highly expected due to the strong jaw movement. The PCL outer boxes which contain the electrode, hydrogel, and hBMSCs seeded on the collagen sponge were implanted into each defect site and the incision sites were then sutured. After the surgery, in Groups 2 and 3, electrical stimulation was applied for 1 week. In the case of Group 3, after 1 week of electrical stimulation, rhBMP-2

(5 μg/defect) was injected into the defect site using a disposable syringe. Four weeks after surgery, the animals were sacrificed and quantitative evaluations of new bone formation were conducted using soft x-ray analysis, micro-CT analysis and histology with H&E staining. Every animal experiment was performed in accordance with the "Recommendations for Handling Regulations for Laboratory Animals for Biomedical Research" compiled by the Committee on the Safety and Ethical Handling Regulation for Laboratory Experiments of the School of Dentistry at Seoul National University

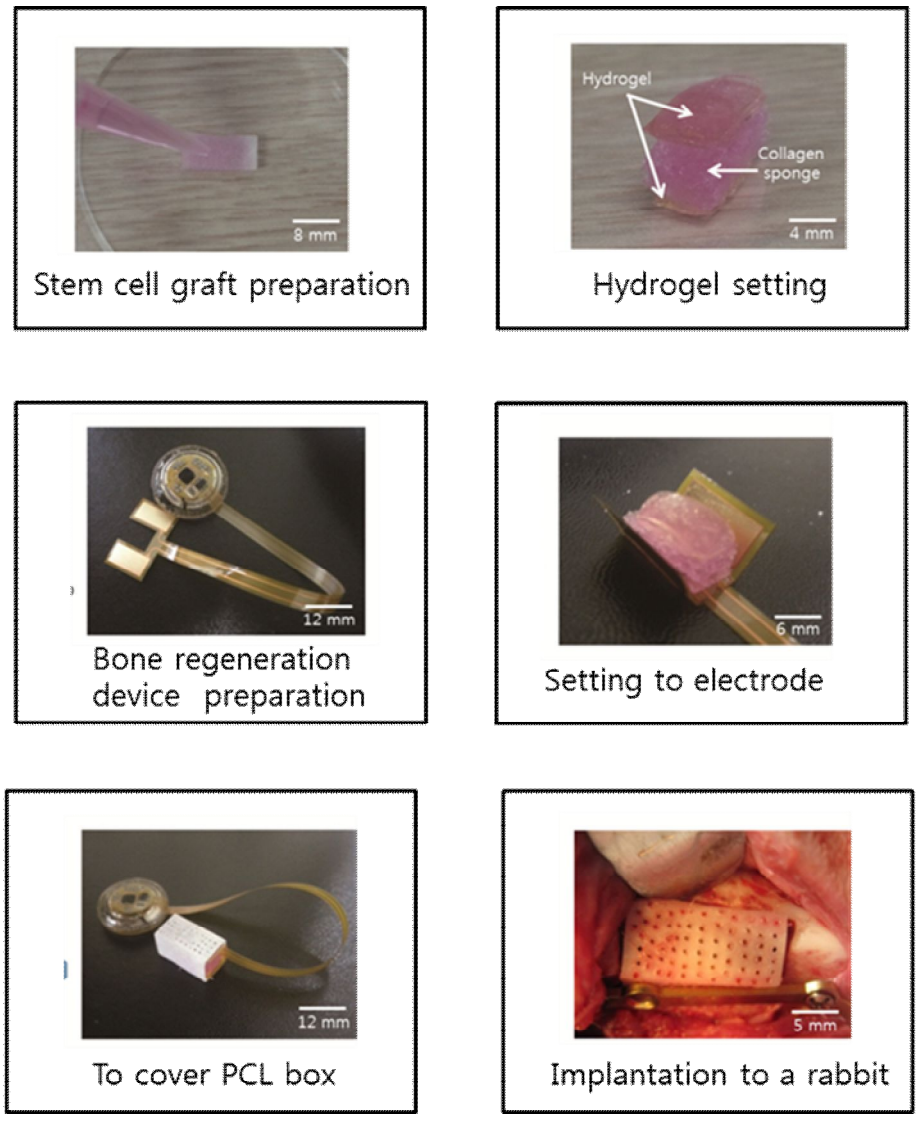

Figure 2.14 The entire process of bone regeneration experiment

2.2.8 Assessment of bone regeneration

2.2.8.1 Soft x-ray

After harvesting the mandibular body, including the defect, a soft x-ray was taken with a cabinet-style soft x-ray unit (CMB-2,

Softex Co. Japan) The radiographic parameters were 30 kVp and 2 mA, the exposure time was 90 seconds.

2.2.8.2 micro CT

The mandibular body including the defect and PCL outer box was harvested from the skull and fixed in 10% formalin for 1 week. Micro CT scans were taken for quantitative evaluations of new bone formation using the SkyScan 1172® microfocus x-ray system (SkyScan, Kontich, Belgium) with CT software of CTAn 1.8®, CTvol, and NRecon reconstruction® (SkyScan). The SkyScan 1172 microfocus x-ray system is equipped with a microfocus x-ray tube with a focal spot of 2 mm, producing a cone beam that is detected by a 12-bit cooled x-ray camera CCD fiber-optically coupled to a 0.5 mm scintillator. The resulting images were 2000 x 1048-pixel square images with an aluminum filter used to produce optimized images. Reconstructions and analyses were performed using NRecon reconstruction and CTAn 1.8 software, respectively. A second-order polynomial correction algorithm was used to reduce the beam-hardening effect for all samples. To measure newly formed bone, a circular area of a pre-defined size was selected as the region of interest (ROI) in two-dimensional images. The pixel zone representing ossification in the defined ROI was then reconstructed in 3D by creating a volume of interest (VOI) in the lower and upper ranges of the threshold using grayscale units. After

using CTAn 1.8 on each reconstructed BMP file, the bone volume, bone density, trabecular thickness, trabecular seperation, and trabecular number were obtained using a CT-analyzer in direct 3D based on a surface-rendered volume model according to the manufacturer's instructions. To measure the bone mineral density, attenuation data for ROI or VOI were converted to Hounsfield units and expressed as a value of the bone mineral density using a phantom (SkyScan). This phantom contained rods of calcium HA (CaHA) having a standard density corresponding to rabbit bone, which ranges from 1.26 to 1.65 g/cm^3. BMD values were expressed in grams per cubic centimeter of CaHA in distilled water. A zero value for bone mineral density corresponded to the density of distilled water alone (no additional CaHA), and a value greater than zero corresponded to non-aerated biologic tissue

2.2.8.3 Histochemical staining

After 3D reconstruction of the micro CT images, the scaffold was decalcified in an ethylenediaminetetraacetic acid solution (7%, pH=7.0) for 3-4 days. The specimens were then dehydrated in 70% ethanol and embedded in paraffin. For histochemical staining, decalcified paraffin sections were cleaned for 10 min with xylene and stained with Masson's trichrome (MT) for the detection of bone structures. Digital images of the stained sections were collected using a transmission and polarized light Axioskop

microscope (Olympus BX51, Olympus Corporation, Tokyo, Japan). The decalcified specimens were cut in the buccolingual direction at the middle height of the bone defect area

2.3 LCP based implantable bone regeneration device

2.3.1 Device configuration

LCP based bone regeneration device has a shape of graft containment system itself so it is able to contain stem cell graft. Also a current generator chip, a pair of electrode for delivery of electrical stimulation to cell graft, an inductive link for power receive from external power transfer device are embedded in the LCP device. Using LCP film, it is possible to make multi-layered structure. LCP film has characteristics of high hermeticity and very low moisture absorption rate. There characteristics of LCP film allow that setting electronics inside the LCP based device. LCP is thermal plastic material so it is easy to make various three dimensional structure by heat treatment. And a high osseointegration property of LCP makes the LCP device as a bone substitute itself. Figure 2.15 is a conceptual art of LCP based implantable bone regeneration device.

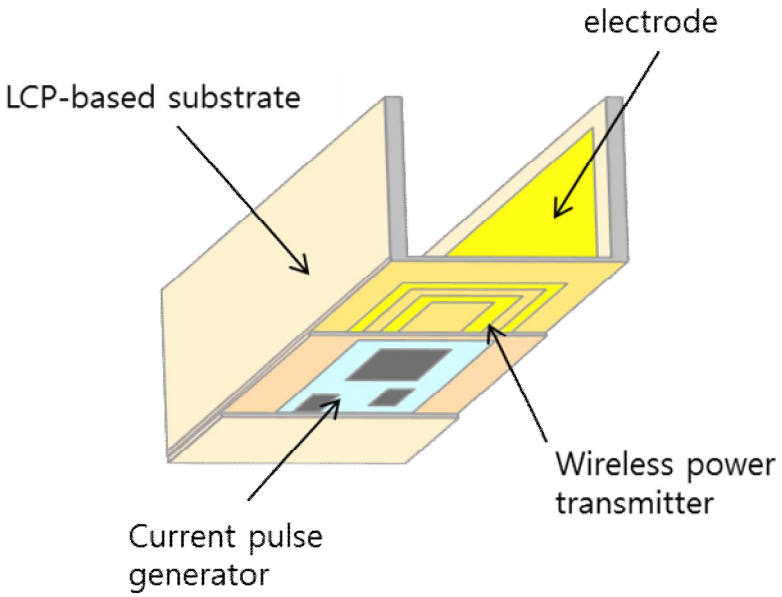

Figure 2.15 A conceptual art of LCP based implantable bone regeneration device

The device is designed as a shape which can be applied to rabbit mandibular defect model. The device dimension is 15 x 7 x 7 mm. It consists of a bottom plate which has an inductive coil and a current generator chip and two sidewalls which have a pair of gold electrode. Between the sidewalls a proper size of cell graft is loaded. Figure 2.16 demonstrates the entire process of producing LCP based bone regeneration device.

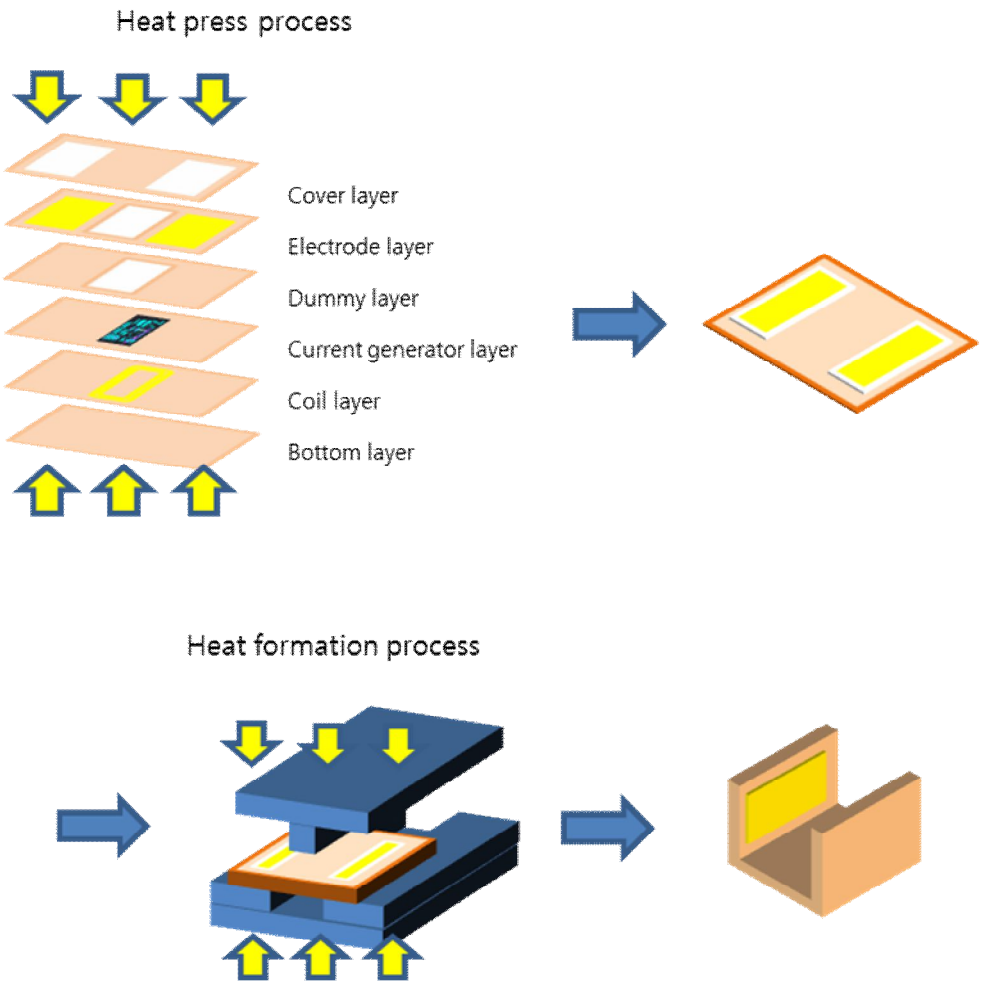

Figure 2.16 The entire process of producing LCP based bone regeneration device

On the each layer of LCP film, electrode, inductive coil and PCB is designed respectively. And all of the film is unitized by heat press process. From the lowest, bottom layer, coil layer, PCB later, electrode layer and cover layer are positioned. And between the each layer there is adhesion layer made by LCP film that melts at lower temperature compare to basic layers. There is dummy layer

that protects chip from heat press process. Through heat press process the unitized LCP films processed in to shape that can contain a cell graft by heat formation process.

2.3.2 LCP layers for bone regeneration device

LCP layer group for bone regeneration device includes electrode layer, inductive coil layer, PCB layer, cover layer, bottom layer, dummy layer and adhesion layer. LCP films that used in this device are two types, CTF and FA. The main difference of two films is melting temperature. CTF is melted at 310 degree and FA is melted at 285 degree, lower temperature than CTF film. The bottom layer, cover layer, coil layer, PCB layer and electrode layer were made by CTF film and other layer is made by FA film. All LCP is offered by Kuraray, Tokyo, Japan.

2.3.2.1 Electrode layer

Electrode layer is produced on CTF film of 50 μm thickness through shadow masking process. To produce the electrode a shadow mask is produced in advance. Figure 2.17 is the feature of the shadow mask produced in advance. A size of the shadow mask is 4 inch. Using this mask, five electrode pair is produced at once.

Figure 2.17 The feature of the shadow mask

After cleaning LCP film, the film is cut in the shape of 4 inch wafer. Then the LCP film is covered by the shadow mask and set into E-gun evaporator. At 10^{-5} torr, 100 nm of titanium and 300 nm of gold thin film are deposited. After removing the shadow mask, electrode layer is completed. Figure 2.18 shows the produced electrode layer.

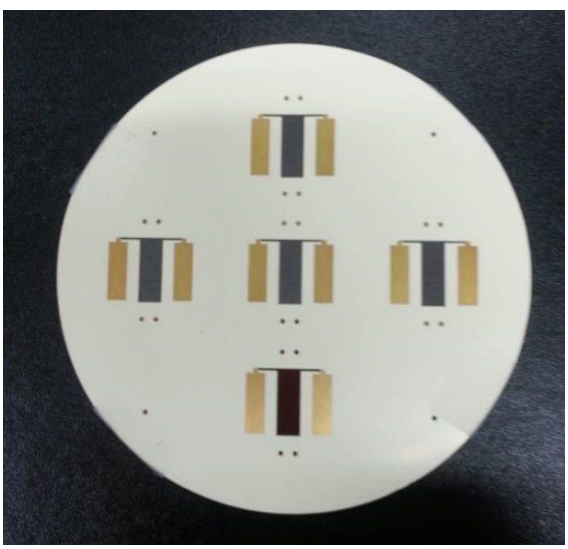

Figure 2.18 The produced electrode layer

2.3.2.2 Inductive coil layer

Inductive coil layer was designed by AutoCad 2011 and produced by outsourcing (Flexcom, Korea). Figure 2.19 is the feature of the designed inductive coil layer.

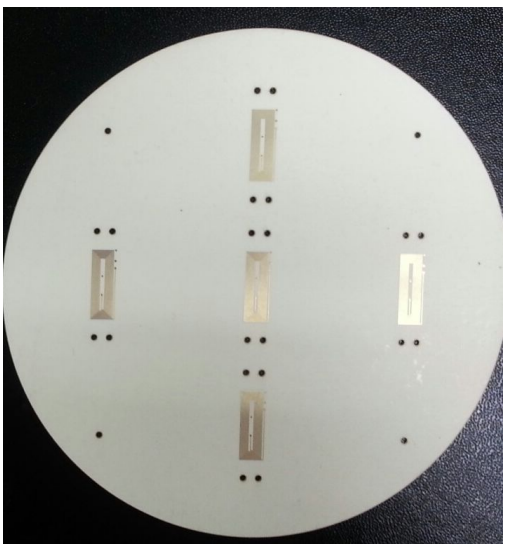

Figure 2.19 The feature of the inductive coil layer

The coil layer is restricted in the bottom plate of LCP device. The size of the bottom plate is 5 mm by 12 mm. This means the coil of LCP device is small and has a low Q-factor. Therefore to gain higher Q-factor, the coil was designed in multi-layered structure. The width of coil line and interval of coil line were 100 μm. Each layer has 6 turns of coil. The entire thickness of the coil layer is 200 μm. Figure 2.20 is the feature of produced inductive coil layer.

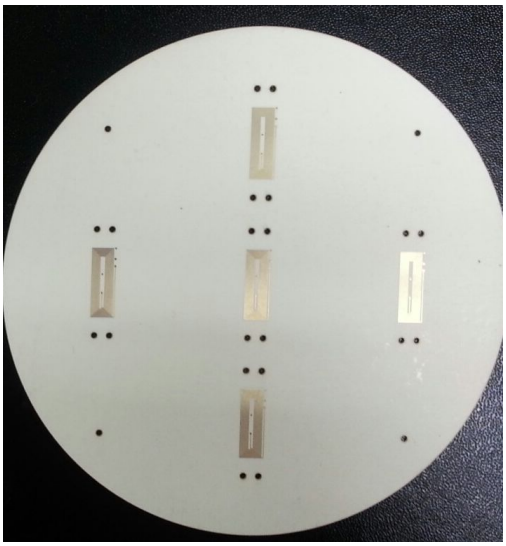

Figure 2.20 The feature of the inductive coil layer

2.3.2.3 PCB layer

Inductive coil layer was designed by AutoCad 2011 and produced by outsourcing (Flexcom, Korea). The thickness of PCB layer is 50 μm. The current generator chip was same chip used in both bioreactor and bone regeneration device. The chip was bonded on PCB layer through wire bonding and external components were assembled. Figure 2.21 demonstrates the produced PCB layer and the PCB layer with bonded chip.

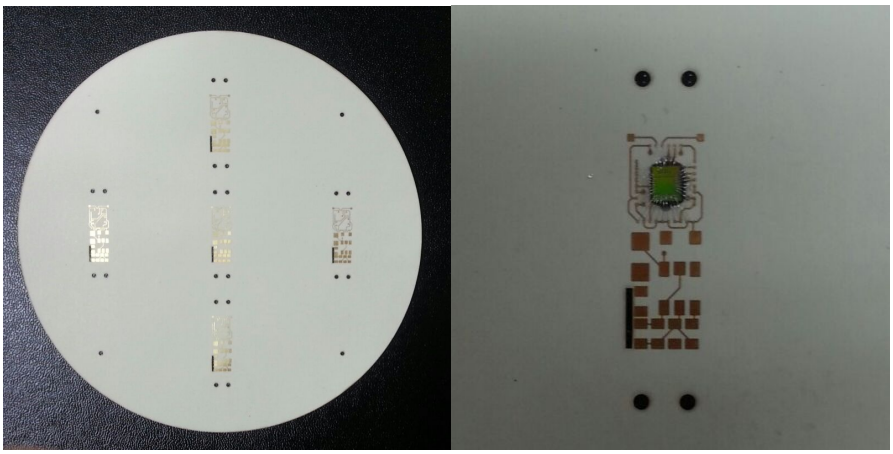

Figure 2.21 PCB layer and wire bonded chip on the layer

2.3.2.4 Other layers

Cover layer and bottom layer were produced in 50 μm of CTF film. These layers are the outmost layer of the bone regeneration device and protect inner layers. Dummy layer is located into between PCB layer and electrode layer so the dummy layer protects the chip and component on the PCB layer from damage by heat press. Adhesion layer was made by 25μm of FA film and was used to attach each layers. Figure 2.22 shows each of layers.

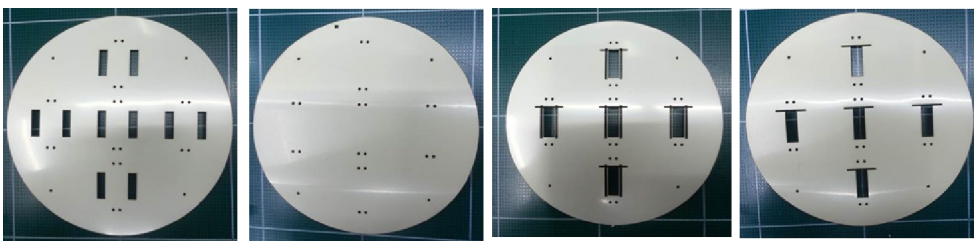

Figure 2.22 LCP layers. Cover layer, bottom layer, dummy layer and adhesion layer in sequence.

2.3.3 Heat press process and heat formation process

Heat press process is conducted to unitize all LCP layers. And through heat formation process, the unitized layers deforms to the shape which is able to contain a cell graft. For both of process, customized aluminum molds were used. Figure 2.23 and 2.24 show two molds for heat press process and heat formation process.

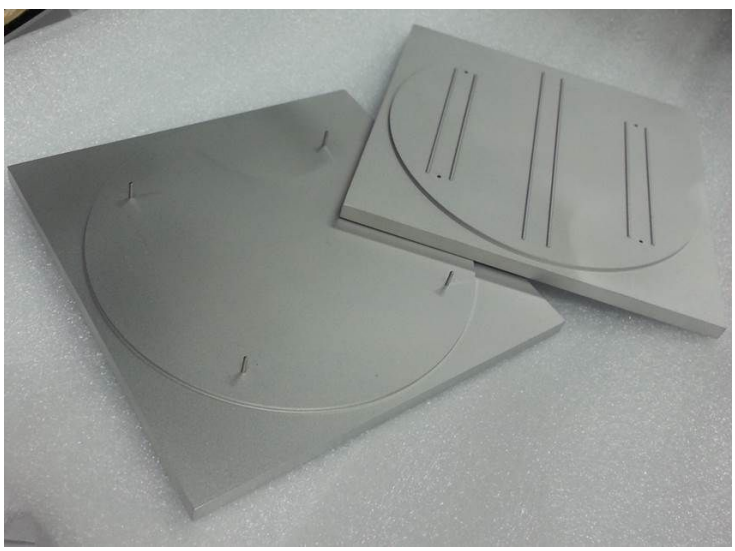

Figure 2.23 The mold for heat press process

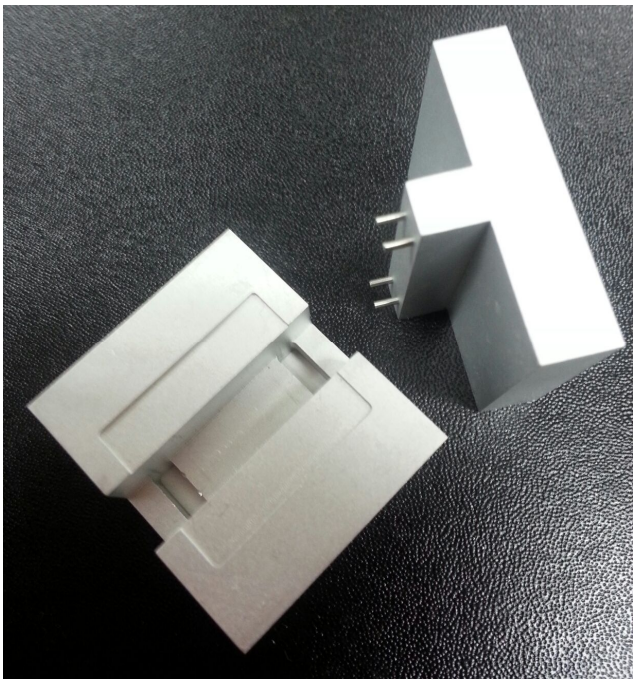

Figure 2.24 The mold for heat formation process

After heat press process, the entire thickness of the LCP device is about 1 mm. This thickness is too thick to deform by heat formation process. It is necessary to make the commissure of the bottom plate and the sidewall thinner than 1 mm. So the mold for hear press process has a 1 mm height of triangular structure. The heat press process procedure is as in the following. First the current stimulator chip and passive components were bonded to the PCB layer using wire bonding method or silver paste. Then every layer etched with O_2 plasma using plasma etcher. The etch process time was 5 minute and the power of plasma was 100 W. By plasma etching, molecular links of LCP film disconnect and this allows easier unitization of each films. After plasma etching, each layer was cleaned by N_2 air gun shower. Every process was conducted in

clean room to prevent micro particle. Before setting LCP layers on the heat press process mold, 1 mm thickness of ceramic paper and 200 μm thickness of Teflon paper were set. The ceramic paper makes uniform pressure to LCP layers and the Teflon paper prevents sticking of FA film which leaks during heat press process. After setting of ceramic paper and Teflon paper, LCP layers were set. Then the mold was set into customized heat press machine, heat press process was executed. The heat press process is conducted at 285 degree with pressure of 200 kg for 30 min. After heat press process the unitized LCP layers was cooled down then cut into the size to be set into the for heat formation mold. The heat formation process also used the customized heat press machine. The heat formation process was conducted at 100 degree with adequate pressure given manually.

Chapter 3 Results

3.1 Cell proliferation results using implantable bioreactor

The proliferation of hMSCs was assessed after *in vivo* cell culture using the implantable bioreactor with titanium electrodes. In the *in vitro* experiments, after one week of BEC stimulation with the parameters of an amplitude of 40 μA, a duration of 100 μs, and a frequency of 100 Hz, the cell growth of the electrically stimulated hMSCs was increased by 19% ($p<0.05$) compared to the unstimulated hMSCs. However, this cell proliferation tendency was not repeated in the *in vivo* experiments using the same type of bioreactor. The cell growth of electrically stimulated hMSCs after one week of BEC stimulation showed a decreasing trend compared to the proliferation of the control group (Figure 3.1).

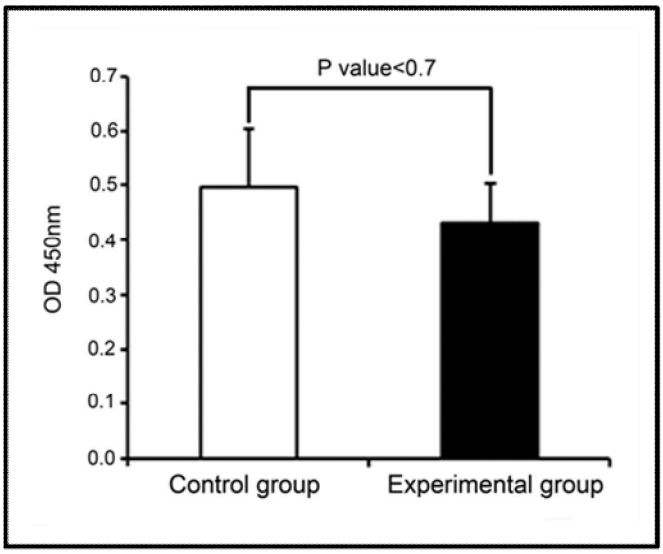

Figure 3.1 Cell proliferation result of the in vivo cell culture using the implantable bioreactor with titanium electrodes

Otherwise, in the experiments using the implantable bioreactor with polyimide electrode, the growth of hMSCs was promoted by BEC. The proliferation of hMSCs showed an increasing tendency, with 22% increase compared to the proliferation result of the unstimulated hMSCs. Figure 3.2 shows the cell proliferation result of the *in vivo* cell culture experiment using the bioreactor with polyimide electrode.

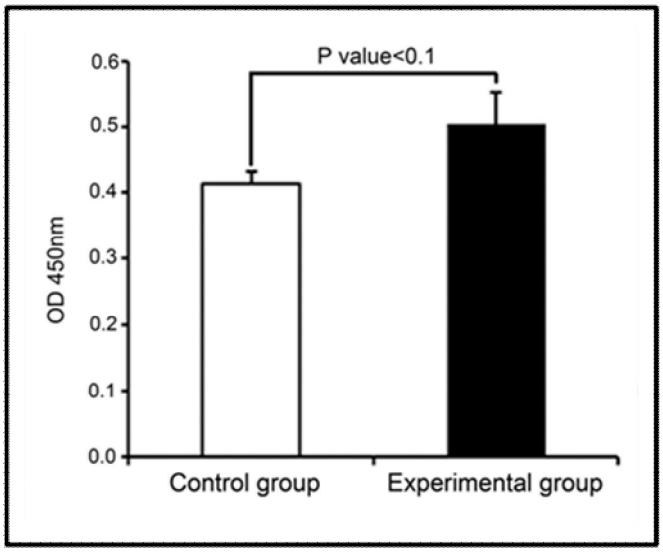

Figure 3.2 Cell proliferation result of the *in vivo* cell culture using the implantable bioreactor with polyimide electrode

The morphological appearance of the hMSCs cultured in the bioreactor with polyimide electrode was observed by SEM. In figure 3.3, cell adhesion forms of the group with electrical stimulation and the group without electrical stimulation. hMSCs were cultured in the collagen sponge for 7 days with electrical stimulation. During the culture period, the pores in the sponge became filled with hMSCs and secreted extracellular matrix to form a matrix layer resulting in the virtual disappearance of the pores. In contrast, the extracellular matrix layer was very rare and the porous collagen structure was more noticeable in the unstimulated group.

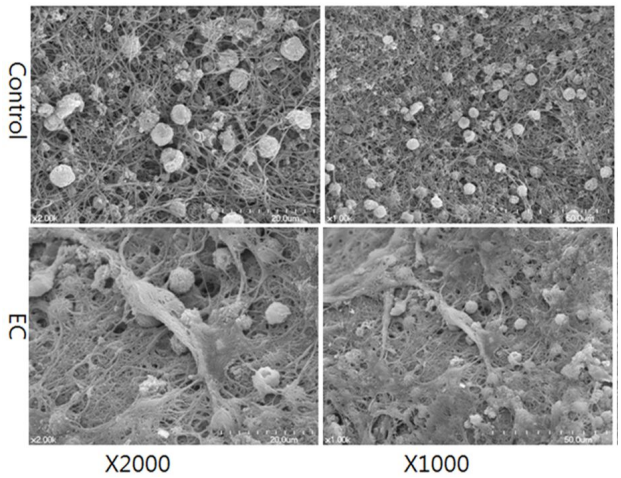

Figure 3.3 Scaled-up features of adhered hMSCs on the collagen sponges

RT-PCR was performed using human-specific primer. The collagen type I gene was expressed higher in the electrically stimulated group in same GAPDH condition. Figure 3.4 shows total RNA extraction results of cell proliferation experiments.

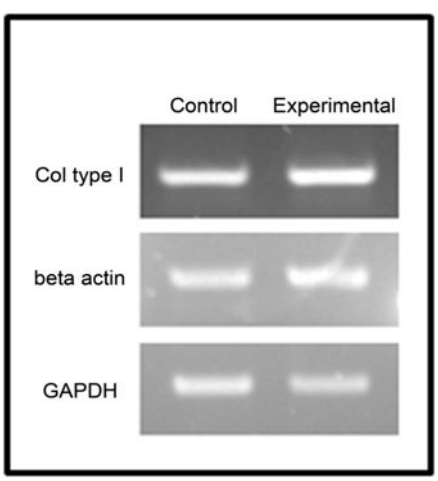

Figure 3.4 Total RNA extraction results of cell proliferation experiments using bioreactor

3.2 Bone regeneration results using bone regeneration device

3.2.1 Radiological and histological examinations

The new bone formation was evaluated from radiological and histological examinations four weeks after surgery in three groups. Figure 3.5A shows the defect site of the rabbit mandible used in this study. Figure 3.5B, C, D is a radiological image of group 1, 2, 3 in sequence respectively and figure 3.5E, F, G is histological image of group 1, 2, 3 in sequence respectively. Figure 3.5B and E is the result of group 1, figure 3.5C, F is the result of group 2 and figure 3.5D, G is the result of group 3. In the radiograms of the three groups, Group 3 showed wider and more enhanced radio-opacity, which represented more new bone formation, compared with Groups 1 and 2. In the histological examination of the MT-stained sections, there was no inflammatory reaction. In Group 1, the hydrogel remained within the bone defect, and new bone was relatively less formed than in Groups 2 and 3. However, in Groups 2 and 3, more abundant new bone could be observed

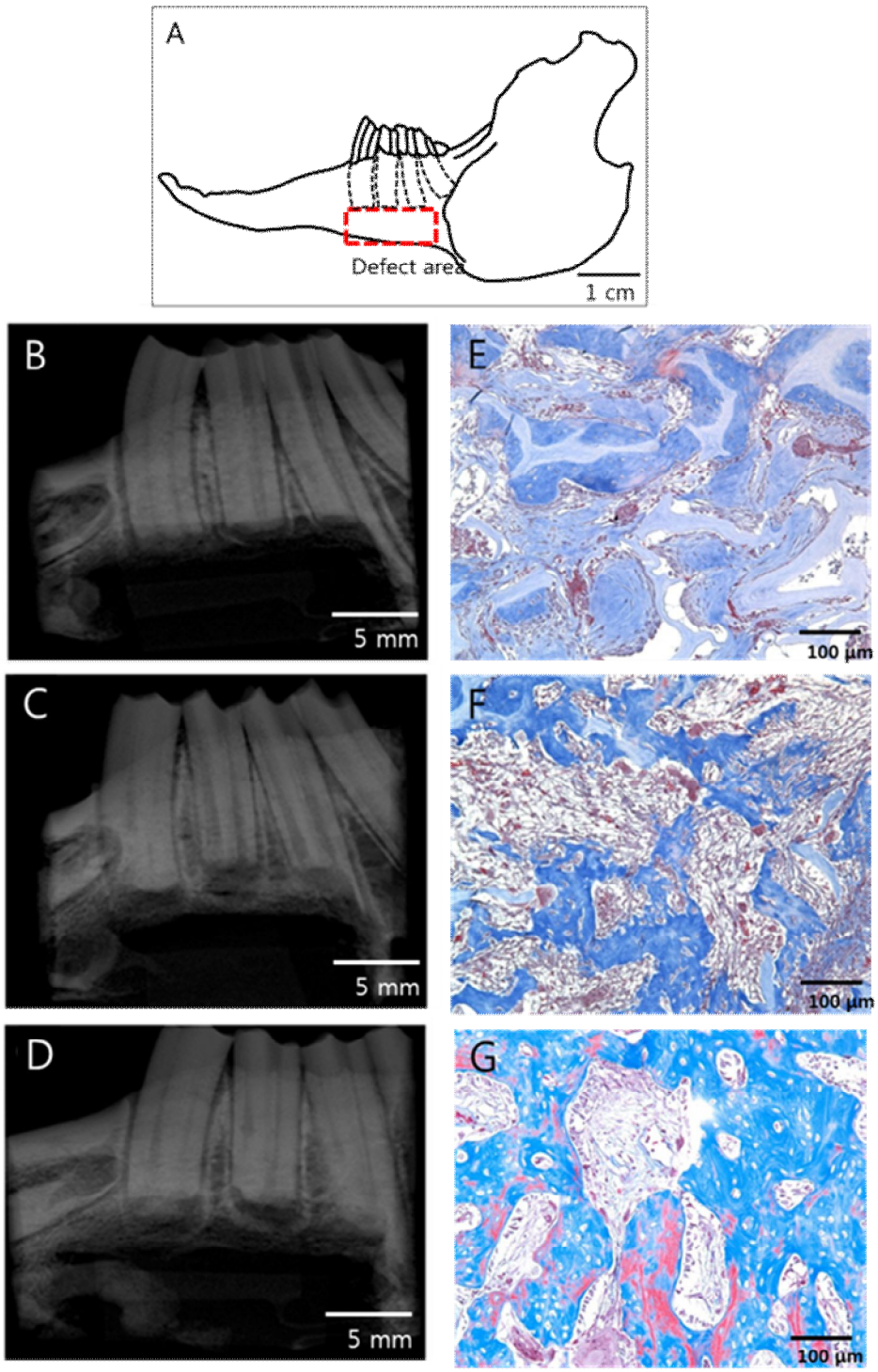

Figure 3.5 The illustration of rabbit mandible defect and radiological and histological images of group 1, 2, 3

3.2.2. Micro CT analysis

The bone structure and new bone formation were evaluated using micro CT software, which calculates morphometric parameters from a selected volume of interest. The morphometric parameters are listed in Table 3.1. Group 2 demonstrated a significant increase in new bone formation compared with Group 1. Group 3 showed a higher new bone formation tendency compared with Group 2. Group 2 showed a higher bone volume by 260% ($p<0.01$) compared with Group 1, and Group 3 showed a higher BV by 442% ($p<0.01$) compared with Group 1. The surface of the new bone normalized to the real defect volume, trabecular numbers, and the degree of connectivity showed a tendency similar to that of bone volume. The bone density of Groups 2 and 3 showed higher fold values of 206% ($p<0.01$) and 296% ($p<0.01$), respectively, compared with Group 1. The trabecular numbers of Groups 2 and 3 showed higher fold values of 220% ($p<0.01$) and 372% ($p<0.01$), respectively, compared with Group 1. The trabecular connectivity in Groups 2 and 3 showed higher fold values of 208% ($p<0.05$) and 284% ($p<0.01$), respectively, compared with Group 1. The trabecular thickness in Groups 2 and 3 showed a higher tendency by ratios of 121% and 117%, respectively, compared with Group 1. The trabecular separation in Group 2 was 95% compared to Group 1, while that in Group 3 was 90% compared with Group 1. The total bone mineral density of Groups 2 and 3 showed higher values with

ratios of 103% ($p<0.01$) and 107.5% ($p<0.01$), respectively, compared with Group 1. The partial bone mineral density of Groups 2 and 3 showed higher values with ratios of 104.9% ($p<0.01$) and 122.4% ($p<0.01$), respectively, compared with Group 1.

Table 3.1 Evaluation and summery of the micro CT analysis

Morphometric Parameters	Fold Value (Ratio to Group 1)	
	Group 2	Group 3
Bone volume	2.6 **	4.42**, ††
Bone density	2.06 **	2.96**, †
Trabecular thickness	1.21	1.17
Trabecular number	2.20 **	3.72 **, ††
Trabecular separation	0.95	0.90
Connectivity	2.08 *	2.84**
Total bone mineral density	1.03**	1.075 **, ††
Partial bone mineral density	1.049**	1.224**, ††

(Significant difference from group 1, *$p<0.05$, **$p<0.01$ and between group 2 and 3, †$p<0.05$, ††$p<0.01$

Chapter 4 Discussion

4.1 Implantable bone regeneration device for bone graft transplantation therapy

In this study, development of an implantable bone regeneration device which is capable to induce electrical stimulation into bone defect is demonstrated. The device is applicable to bone graft transplantation. Using this device, bone regeneration was evaluated. For the development of the bone regeneration device, an implantable bioreactor that can culture stem cell grafts using electrical stimulation in *in vivo* bioreactor circumstance was developed as first step. The electrodes used in the bioreactor were titanium electrode pair and polyimide electrode. The flexible polyimide electrode can deliver electrical stimulation effectively to local three-dimensional tissue by changing the shape of the electrode fitting to the target tissue. Therefore the bone regeneration device for rabbit mandible defect model was produced by improving the bioreactor device with polyimide electrode. And using this device, bone regeneration experiment combined treatment of electrical stimulation and injection of growth factor, BMP-2 was executed. The produced device in this study had a pair of flexible polyimide electrode shaped a plate form and the device could deliver electrical stimulation to three-dimensional bone defect site or entire of bone graft through effect of electric field

unlike conventional bone regeneration device. By using the flexible electrode the device in this study can be used in not only rabbit mandible defect model but also in various forms of bone defect model and the defect has three-dimensional area. Also this device can be applied to deliver electrical stimulation locally into bone graft for bone regeneration and various biological tissues.

4.2 Selection of the electrical stimulation parameters

Electrical stimulation regulates cell membrane potential in form of ionic current. Then regulated membrane potential activates voltage-gated calcium channel. From the event, intracellular calcium concentration increases, then calcium/calmodulin pathway is activated. As the result, electrical stimulation induces secretion of cytokine which is necessary for proliferation and differentiation of osteoblast cell and accelerates bone mineralization. Furthermore the used electrical stimulation is activated cellular process of stem cells and helps in cell proliferation and bone regeneration from the results of *in vivo* cell proliferation experiment using the implantable bioreactor and the bone regeneration device. However, the electrical stimulation parameters for *in vivo* bone regeneration should be set carefully.

According to parameter of electrical stimulation, it is possible that the creation of reactive oxygen species through an oxidation reduction process due to the Faradaic reaction near the electrode

rather than encouragement of bone repair. Also too high strength of the electric field may lead to cell damage by Joule heating effect. Improper stimulation parameters can cause bone resorption, rather bone regeneration. The electrical stimulation parameters used in this study was bi-phasic charge-balanced current stimulation. The charge-balanced BEC pulse stimulation has some advantages compare with voltage stimulation. The charge delivered to the cell in the form of ionic current is important factor for regulation of cellular process. In case of the voltage stimulation, the amount of delivered charge changes according to the status of electrode even though constant voltage is applied. However in case of current stimulation, unless varying the impedance between cell and electrolyte significantly, it is possible to deliver a constant charge regardless of the status of electrode. This means that safe and reliable electrical stimulation is possible in the range of generating cellular processes. In addition the current stimulation strategy using charge-balanced pulse can suppress pH changes due to charge accumulation and the creation of reactive oxygen species. So it is possible that preventing electrode corrosion and cell damage. Furthermore it was reported in previous study of bone regeneration using rabbit that the current pulse of 10~20 μA is effective in bone regeneration [77]. The conventional bone regeneration devices use that current pulse parameter [56]. The stimulation parameters used in this study were the parameters that augment cell proliferation and improve the cell viability of hBMSCs [4]. Also, these parameters had the obvious effect of increasing cell proliferation,

up-regulating ALP, IGF-1 and TGF-beta1 and causing the early-stage induction of VEGF, which is necessary for bone formation. From these preliminary inspections, the stimulation parameter was set and through this parameter the results of cell proliferation and bone regeneration were obtained.

4.3 An alternative tissue engineering method of in situ stem cell therapy using intracorporeal cell culture

In this study bone regeneration was conducted using combined treatment of stem cell graft, hydrogel, collagen sponge and PCL in *in vivo* bioreactor circumstance using electrical stimulation. Especially the produced bone regeneration device allows simultaneous use of electrical stimulation and growth factor which were important morphogenetic signals for improvement of bone formation. So this device can be applied with *in situ* stem cell application and intracorporeal cell expansion. The characteristic of this regeneration strategy follows. First, in this strategy, the regeneration is conducted by cell culture at *in vivo* bioreactor circumstance, so the stem cell can be used at surgery just after harvest stem cell without long period of *in vitro* cell culture about more than a month. Through this method, it is possible that reduction of cell culture period, cost for cell culture and risk of infection. Also enhanced survive of injected stem cell is expected by up-regulated cell viability. Second, through this strategy, it is

possible that regulation of growth factor and electrical stimulation at *in vivo*. Although cell culture circumstance with cellular process regulation is the characteristic of *in vitro* cell culture method, using this device and strategy the advantage of cellular process regulation is expected even in *in vivo* culture. Therefore, the method of delivering electrical stimulation at the stage of new bone formation can overcome the obstacles of fewer stem cells for large bone defects, leading to the expectation of better bone regeneration. This study is thus a preliminary study of an alternative tissue engineering method that can avoid shortcomings such as a long cell culture period, a high cost and an increased risk of infection from the extracorporeal *in vitro* cell culturing processes used in ordinary tissue engineering. The method promotes cell expansion and induces tissue repair by seeding promptly separated stem cells from the blood of bone marrow on a scaffold of a collagen sponge followed by implantation into the tissue defect area in conjunction with electrical stimulation

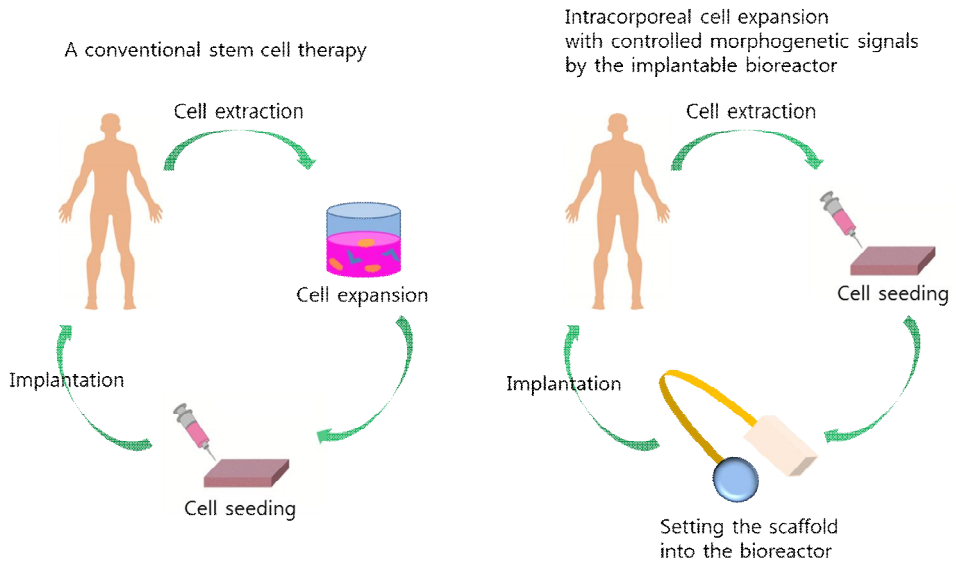

Figures 4.1 Concept of the conventional tissue regeneration therapy using *in vitro* cell culture and the intracorporeal cell culture

4.4 Transfer of electrical stimulation according to electrode design of bioreactor

There is no difference but the shape of electrode between the bioreactor with the pair of titanium electrodes and the bioreactor with the polyimide electrode. But in the cell proliferation results of *in vivo* cell culture experiment, a contrast tendency was observed. The obvious cell proliferation result was gained at *in vitro* experiment using same stimulation parameters. So the result from the experiment with titanium electrode was an unexpected result. From the result of cell proliferation using titanium electrode did not have a high significance, it may be supposed that the transfer of

electrical stimulation using titanium electrodes was not sufficient. First of all, the titanium electrode uses a tungsten wire for connection between the electrode and the power supply device. For the electrode and the wire were connected by the pair of volt and nut without welding or soldering so there was possibility of a connection line break or an insufficient connection. Moreover as shown in figure 4.2, in the case of titanium electrode, the electrodes are exposed at the outside of the chamber but the inside of chamber, the current path which flows along to the outside of the chamber may be formed by these exposed electrodes. From this, the electrical stimulation which should be concentrated to the cell graft inside of the chamber could be distributed to outside of the chamber. Also the collagen sponge has a higher electrical impedance compare with the muscle. So the current path might be formed along to the outside of the chamber and the cell was not affected by electrical stimulation sufficiently. Therefore, when delivering electrical stimulation to the selected target, the design of the electrode should be considered carefully in order to be delivered the most part of the electrical stimulation to targeted site.

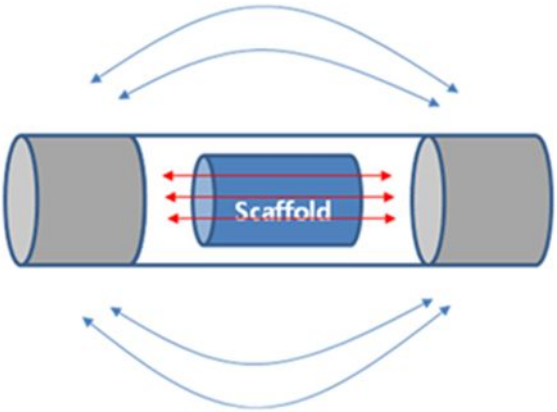

Figure 4.2 The current pathway in the bioreactor using titanium electrodes

4.5 Bone regeneration effect on combined treatment of electrical stimulation and BMP-2

From the bone parameters determined by micro CT, there was a significant increase of new bone formation in the group applied complex treatment of electrical stimulation and BMP-2 compared with the group applied BMP-2 only. The difference between the two groups was caused by the existence of the electrical stimulation. Therefore, it is clear that the different elevation of the bone regeneration between two groups was derived from the electrical stimulation. From the differences in the bone parameters according to treatment time of BMP-2, finding the most effective application time of rhBMP-2 is regarded as important for the acceleration of bone formation combined with electrical stimulation. A better new bone formation trend was obtained in the case of

direct injection of rhBMP-2 to the defect site after electrical stimulation compared with a sustained release of rhBMP-2 to the defect site during hydrogel degradation. In figure 4.3, the conceptual process for the different proliferation and differentiation of stem cells. BMP-2 acts by promoting cell differentiation whereas cell proliferation effect of BMP-2 is small [81]. Electrical stimulation helps stem cell proliferation, cytokine release and growth factor induction. While stem cells differentiate to osteoblasts directly instead of proliferating via BMP-2 despite the use of electrical stimulation. Better new bone formation results in Group 3 were noted compared to those of Group 2. The effect of cell proliferation by electrical stimulation was decreased due to the differentiation of stem cells by the gradually released BMP from the hydrogel carrier. In contrast, in Group 3, plenty of stem cells proliferated by electrical stimulation were differentiated more into osteoblasts compared to the cells in Group 2 when BMP-2 was injected after electrical stimulation. Therefore, when using a combined treatment of electrical stimulation and rhBMP-2, an improvement of new bone formation can be expected when electrical stimulation for cell expansion comes first and rhBMP-2 application follows instead of a sustained release of BMP-2 through a hydrogel carrier.

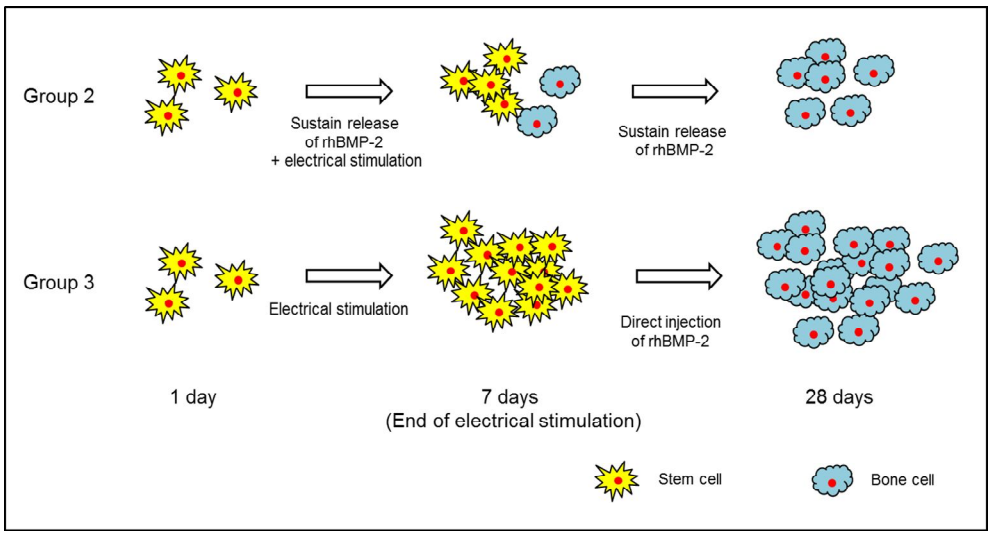

Figure 4.3 The conceptual process for the different proliferation and differentiation of stem cells

4.6 Potential for chronic bone substitute of LCP-based bone regeneration device LCP

Although the designed bone regeneration device was effective for bone healing using bone graft transplantation, there are some parts should be improved. First the bioreactor and bone regeneration device use a battery for power supply to current stimulator. So there are limitations for the setting of parameters, amplitude, duration, and frequency and stimulation period of the electrical stimulation. And the hermeticity of silicone rubber is lower than the hermeticity of metal or ceramic and the silicone package. And the electrodes are not packaged as a monolithic material. Therefore if the device is implanted for long period, there is a risk of the penetration of body fluid into the device and this may occur a failure

of the device or infection through toxic product from the corroded device. Furthermore the current stimulator and battery were packaged together the implant package became large. From the size of the package, the bioreactor part and the package part were separated and connected by long connection line and it is required for additional surgery for implantation of the connection line and extraction of the device after healing. From these limitations, the requirements for the implantable device for bone regeneration are suggested. First, in the setting of stimulation parameter flexibility is required. Second, the package of current stimulator should be hermetic to prevent a failure of electronics by a body fluid penetration or dissolution of the packaging material during implanted period. Last, the bioreactor itself should have a high osteointegrity because the device is used for bone regeneration and the device remains in the body. Therefore the LCP based implantable bioreactor device can be used as improved bone regeneration device that overcome the limitations mentioned above. There are some advantages using the suggested LCP-based bone regeneration device. First, utilizing the characteristic of LCP film that allows multi-layered structure, it is possible that current stimulator and inductive link for power receive can be combined in bioreactor. Second, power is delivered by inductive link so electrical parameter can be selected with flexibility. Third, LCP is implantable for long term without failure of electronics inside of the package and infection through electronics because it has very inert chemical reactivity and very low moisture absorption. Fourth, the

LCP is highly osseo-integratable itself, so LCP bioreactor can be used as bone substitute itself. From these characteristics, the LCP-based bone regeneration device provides a bioreactor circumstance embedded an electrical stimulation device and it can act a chronic bone substitute. Also after bone regeneration through additional electrical stimulation, an optional bone management is possible.

Chapter 5 Conclusion

In the present study, the implantable bioreactor and bone regeneration device using electrical stimulation that can be applied to stem cell grafting were developed. Using the bioreactor device, cell proliferation and up-regulation of cell viability were achieved. The bone regeneration experiment using the bone regeneration device, new bone formation was increased. Also LCP based bone regeneration device is introduced as an improved implantable bone regeneration device. The device in this study can be used an intracorporeal cell culture platform, so it can be alternative of cell culture system that overcome limitations of conventional cell culture system. The device introduced in this study suggested to several limitations of conventional implantable bone regeneration device. The bone regeneration device is feasible to be applied in three dimensional bone grafting. As an "All in one device", LCP device does not need additional surgery. It acts electrical stimulator, bone substitute and graft containment system. For future work, stimulation parameter regulation using data telemetry and various shape of bone regeneration device can be used to various bone defect are expectable.

References

[1] An, Soon Kwan, et al. "Design for a simplified cochlear implant system." *Biomedical Engineering*, IEEE Transactions on 54.6 (2007): 973-982.

[2] Jeong, Joonsoo, et al. "Liquid Crystal Polymer(LCP), an Attractive Substrate for Retinal Implant." *Sensors and Materials* 24.4 (2012): 189-203.

[3] Kim, Jaehyung, et al. "VPL-DBS on neuropathic pain rat model is effective in mechanical allodynia than cold allodynia." *Neurological Sciences* 33.6 (2012): 1265-1270.

[4] Kim, In Sook, et al. "Novel effect of biphasic electric current on in vitro osteogenesis and cytokine production in human mesenchymal stromal cells." *Tissue Engineering Part A* 15.9 (2009): 2411-2422.

[5] Lee, Tae Hyung, et al. "Functional Regeneration of a Severed Peripheral Nerve With a 7-mm Gap in Rats Through the Use of An Implantable Electrical Stimulator and a Conduit Electrode With Collagen Coating." Neuromodulation: *Technology at the Neural Interface* 13.4 (2010): 299-305.

[6] Zhou, David D., and Elias Greenbaum. *Implantable Neural Prostheses*. Dordrecht: Springer Verlag, 2009.

[7] 오승모, 전기화학, 자유아카데미, 2010

[8] Allen, J. Bard, and R. Faulkner Larry. "Electrochemical methods: fundamentals and applications." *Department of Chemistry and Biochemistry University of Texas at Austin, John Wiley & Sons, Inc* (2001).

[9] Enderle, John Denis, and Joseph D. Bronzino, eds. *Introduction to biomedical engineering*. Academic Press, 2012.

[10] Urry, Lisa A., et al. *Campbell biology*. Boston: Pearson, 2011.

[11] http://education-portal.com/academy/lesson/lipid-bilayer-definition-structure-function.html#lesson

[12] Hille, Bertil. *Ion channels of excitable membranes*. Vol. 507. Sunderland, MA: Sinauer, 2001.

[13] Kandel, Eric R., James H. Schwartz, and Thomas M. Jessell, eds. *Principles of neural science*. Vol. 4. New York: McGraw-Hill, 2000.

[14] Junge, D. "Nerve and Muscle Excitation. 2nd." *Ed., Sunderland,*

MA: Sinauer (1981).
[15] Purves, Dale, et al. "Channels and Transporters." *Neuroscience (2nd ed.)* (2001).
[16] Connolly, C. N., and K. A. Wafford. "The Cys-loop superfamily of ligand-gated ion channels: the impact of receptor structure on function." *Biochemical Society Transactions* 32.Pt3 (2004): 529-534.
[17] Matulef, Kimberly, and William N. Zagotta. "Cyclic nucleotide-gated ion channels." *Annual review of cell and developmental biology* 19.1 (2003): 23-44.
[18] Kamkin, Andre, Kiselava, Irina. "*Mechanosensitive ion channels*." Springer (2008).
[19] Boriek, Aladin M., and Ashok Kumar. "Regulation of intracellular signal transduction pathways by mechanosensitive ion channels." *Mechanosensitive Ion Channels*. Springer Netherlands, 2008. 303-327.
[20] Gu, Yuanzheng, and Chen Gu. "Physiological and Pathological Functions of Mechanosensitive Ion Channels." *Molecular neurobiology* (2014): 1-9.
[21] Tang, Yuye, et al. "A finite element framework for studying the mechanical response of macromolecules: application to the gating of the mechanosensitive channel MscL." *Biophysical journal* 91.4 (2006): 1248-1263.
[22] Bamann, Christian, et al. "Structural guidance of the photocycle of channelrhodopsin-2 by an interhelical hydrogen bond." *Biochemistry* 49.2 (2009): 267-278.
[23] Dhaka, Ajay, Veena Viswanath, and Ardem Patapoutian. "Trp ion channels and temperature sensation." *Annu. Rev. Neurosci.* 29 (2006): 135-161.
[24] Zheng, Jie. "Molecular mechanism of TRP channels." *Comprehensive Physiology* (2013).
[25] Voets, Thomas, et al. "The principle of temperature-dependent gating in cold-and heat-sensitive TRP channels." *Nature* 430.7001 (2004): 748-754.
[26] Brauchi, Sebastian, Patricio Orio, and Ramon Latorre. "Clues to understanding cold sensation: thermodynamics and electrophysiological analysis of the cold receptor TRPM8." *Proceedings of the National Academy of Sciences of the United States of America* 101.43 (2004): 15494-15499.
[27] Yang, Fan, et al. "Thermosensitive TRP channel pore turret is part of the temperature activation pathway." *Proceedings of the National Academy of Sciences* 107.15 (2010): 7083-7088.
[28] Barnett, Mark W., and Philip M. Larkman. "The action

potential." *Practical neurology* 7.3 (2007): 192-197.
[29] http://en.wikipedia.org/wiki/Action_potential
[30] McKinsey, Timothy A., Chun Li Zhang, and Eric N. Olson. "MEF2: a calcium-dependent regulator of cell division, differentiation and death." *Trends in biochemical sciences* 27.1 (2002): 40-47.
[31] http://lsresearch.thomsonreuters.com/maps/550/
[32] Im, Sin-Hyeog, and Anjana Rao. "Activation and deactivation of gene expression by Ca2+/calcineurin-NFAT-mediated signaling." *Molecules and cells* 18.1 (2004): 1-9.
[33] Asahi, Michio, et al. "Physical interactions between phospholamban and sarco (endo) plasmic reticulum Ca2+-ATPases are dissociated by elevated Ca2+, but not by phospholamban phosphorylation, vanadate, or thapsigargin, and are enhanced by ATP." *Journal of Biological Chemistry* 275.20 (2000): 15034-15038.
[34] Reiken, Steven, et al. "PKA phosphorylation activates the calcium release channel (ryanodine receptor) in skeletal muscle defective regulation in heart failure." *The Journal of cell biology* 160.6 (2003): 919-928.
[35] Brad M, Isaacson, et al. "Bioelectric analyses of an osseointegrated intelligent implant design system for amputees." *Journal of Visualized Experiments* 29 (2009).
[36] Ercan, Batur, and Thomas J. Webster. "The effect of biphasic electrical stimulation on osteoblast function at anodized nanotubular titanium surfaces." *Biomaterials* 31.13 (2010): 3684-3693.
[37] Griffin, Michelle, and Ardeshir Bayat. "Electrical stimulation in bone healing: critical analysis by evaluating levels of evidence." *Eplasty* 11 (2011).
[38] Hronik-Tupaj, Marie, et al. "Osteoblastic differentiation and stress response of human mesenchymal stem cells exposed to alternating current electric fields." *Biomedical engineering online* 10.1 (2011): 9.
[39] Dubey, Ashutosh Kumar, Shourya Dutta Gupta, and Bikramjit Basu. "Optimization of electrical stimulation parameters for enhanced cell proliferation on biomaterial surfaces." *Journal of Biomedical Materials Research Part B: Applied Biomaterials* 98.1 (2011): 18-29.
[40] Balint, Richard, Nigel J. Cassidy, and Sarah H. Cartmell. "Electrical stimulation: a novel tool for tissue engineering." *Tissue Engineering Part B: Reviews* 19.1 (2012): 48-57.
[41] Boonrungsiman, Suwimon, et al. "The role of intracellular calcium phosphate in osteoblast-mediated bone apatite formation."

Proceedings of the National Academy of Sciences 109.35 (2012): 14170-14175.
[42] Friedenberg, Z. B., M. C. Harlow, and C. T. Brighton. "Healing of nonunion of the medial malleolus by means of direct current: a case report." *Journal of Trauma-Injury, Infection, and Critical Care* 11.10 (1971): 883-885.
[43] Dwyer, A. F., and G. G. Wickham. "Direct current stimulation in spinal fusion." *The Medical journal of Australia* 1.3 (1974): 73.
[44] Brighton, Carl T., et al. "Direct-current stimulation of non-union and congenital pseudarthrosis. Exploration of its clinical application." *The Journal of Bone & Joint Surgery* 57.3 (1975): 368-377.
[45] Jorgensen, Torben Ejsing. "Electrical stimulation of human fracture healing by means of a slow pulsating, asymmetrical direct current." *Clinical orthopaedics and related research* 124 (1977): 124-127.
[46] Lavine, Leroy S., Irving Lustrín, and Morris H. Shamos. "Treatment of congenital pseudarthrosis of the tibia with direct current." *Clinical orthopaedics and related research* 124 (1977): 69-74.
[47] KANE, WILLIAM J. "Direct current electrical bone growth stimulation for spinal fusion." *Spine* 13.3 (1988): 363-365.
[48] Steinberg, M. E., et al. "Early results in the treatment of avascular necrosis of the femoral head with electrical stimulation." *The Orthopedic clinics of North America* 15.1 (1984): 163-175.
[49] Cundy, P. J., and D. C. Paterson. "A ten-year review of treatment of delayed union and nonunion with an implanted bone growth stimulator." *Clinical orthopaedics and related research* 259 (1990): 216-222.
[50] Cohen, M., A. Roman, and J. E. Lovins. "Totally implanted direct current stimulator as treatment for a nonunion in the foot." *The Journal of foot and ankle surgery: official publication of the American College of Foot and Ankle Surgeons* 32.4 (1992): 375-381.
[51] Brighton, Carl T. "The treatment of nonunions with electricity." *The Journal of Bone & Joint Surgery* 63. (1981):847-51.
[52] Steinberg, Marvin E., et al. "Treatment of avascular necrosis of the femoral head by a combination of bone grafting, decompression, and electrical stimulation." *Clinical orthopaedics and related research* 186 (1984): 137-153.
[53] Lavine, L. S., et al. "The influence of electric current on bone regeneration in vivo." *Acta Orthopaedica* 42.4 (1971): 305-314.

[54] Kahanovitz, Neil. “Electrical Stimulation and Spinal Fusion.” *US Musculoskeletal Review* (2007):36-38.

[55] Paterson, Dennis. "Treatment of nonunion with a constant direct current: a totally implantable system." *The Orthopedic clinics of North America* 15.1 (1984): 47-59.

[56] http://www.biomet.com

[57] Klokkevold, Perry R., and Sascha A. Jovanovic. "Advanced implant surgery and bone grafting techniques." *Carranza's Clinical Periodontology, 9th Edition. Philadelphia: WB Saunders Co* (2002): 907-8.

[58] http://en.wikipedia.org/wiki/Bone_grafting

[59] Chin, Martin, and Bryant A. Toth. "Distraction osteogenesis in maxillofacial surgery using internal devices: review of five cases." *Journal of Oral and Maxillofacial Surgery* 54.1 (1996): 45-53.

[60] Stricker, Andres. “Bone Splitting as a Transversal Augmentation Method for Optimizing the Implant Bed.” *B Braun sharing expertise Aesculap Dental.* (2013)

[61] Cancedda, Ranieri, Paolo Giannoni, and Maddalena Mastrogiacomo. "A tissue engineering approach to bone repair in large animal models and in clinical practice." *Biomaterials* 28.29 (2007): 4240-4250.

[62] Rupani, Asha, R. Balint, and S. H. Cartmell. "Osteoblasts and their applications in bone tissue engineering." *Cell Health and Cytoskeleton* 4 (2012): 49-61.

[63] Geiger, M., R. H. Li, and W. Friess. "Collagen sponges for bone regeneration with rhBMP-2." *Advanced drug delivery reviews* 55.12 (2003): 1613-1629.

[64] Berner, Arne, et al. "Treatment of long bone defects and non-unions: from research to clinical practice." *Cell and tissue research* 347.3 (2012): 501-519.

[65] Katagiri, Takenobu, et al. "Bone morphogenetic protein-2 converts the differentiation pathway of C2C12 myoblasts into the osteoblast lineage." *The Journal of cell biology* 127.6 (1994): 1755-1766.

[66] Kim, Jung Hoon, et al. "An implantable electrical bioreactor for enhancement of cell viability." *Engineering in Medicine and Biology Society, EMBC, 2011 Annual International Conference of the IEEE*. IEEE, 2011.

[67] Lee, Seung Woo, et al. "Monolithic encapsulation of implantable neuroprosthetic devices using liquid crystal polymers." *Biomedical Engineering, IEEE Transactions on* 58.8 (2011): 2255-2263.

[68] Min, Kyou Sik, et al. "A Liquid Crystal Polymer-Based Neuromodulation System: An Application on Animal Model of Neuropathic Pain." *Neuromodulation: Technology at the Neural Interface* 17.2 (2014): 160-169.
[69] Jeong, Joonsoo, et al. "A novel multilayered planar coil based on biocompatible liquid crystal polymer for chronic implantation." *Sensors and Actuators A: Physical* 197 (2013): 38-46.
[70] Lee, Sung Eun, et al. "A flexible depth probe using liquid crystal polymer." *Biomedical Engineering, IEEE Transactions on* 59.7 (2012): 2085-2094.
[71] Kettunen, Jukka, et al. "The fixation properties of carbon fiber-reinforced liquid crystalline polymer implant in bone: An experimental study in rabbits." *Journal of biomedical materials research* 56.1 (2001): 137-143.
[72] Kettunen, J., et al. "Mechanical properties and strength retention of carbon fibre-reinforced liquid crystalline polymer (LCP/CF) composite: An experimental study on rabbits." *Biomaterials* 19.14 (1998): 1219-1228.
[73] Lee, Tae Hyung, and Kim, Sung June. "Implantable multichannel stimulating circuit for neural stimulator." *The 16th Korean conference on semiconductors*, 2009.
[74 Kim, Junghoon, et al. "Enhanced regeneration of rabbit mandibular defects through a combined treatment of electrical stimulation and rhBMP-2 application." *Medical & biological engineering & computing* 51.12 (2013): 1339-1348.
[75] Yang, Seungwon, et al. "Mechanisms by which the inhibition of specific intracellular signaling pathways increase osteoblast proliferation on apatite surfaces." *Biomaterials* 32.11 (2011): 2851-2861.
[76] Lee, Yun-Jung, Jea Seung Ko, and Hyun-Man Kim. "The role of cell signaling defects on the proliferation of osteoblasts on the calcium phosphate apatite thin film." *Biomaterials* 27.20 (2006): 3738-3744.
[77] Yonemori, K., et al. "Early effects of electrical stimulation on osteogenesis." *Bone* 19.2 (1996): 173-180.
[78] Cogan, Stuart F. "Neural stimulation and recording electrodes." *Annu. Rev. Biomed. Eng.* 10 (2008): 275-309.
[79] Chang, Marvin G., et al. "Proarrhythmic potential of mesenchymal stem cell transplantation revealed in an in vitro coculture model." *Circulation* 113.15 (2006): 1832-1841.
[80] Cho, Sungbo, and Hagen Thielecke. "Electrical characterization of human mesenchymal stem cell growth on microelectrode."

Microelectronic Engineering 85.5 (2008): 1272-1274.
[81] Fromigue, O., P. J. Marie, and A. Lomri. "Bone morphogenetic protein-2 and transforming growth factor-β2 interact to modulate human bone marrow stromal cell proliferation and differentiation." *Journal of cellular biochemistry* 68.4 (1998): 411-426
.

국문 초록

전기 자극은 이오닉 커런트의 형태로 세포의 막전위를 변화시킴으로 세포의 세포 활동을 조절시킨다. 전기 자극은 세포의 증식률과 건강도를 향상시키는 효과가 있으며, 높은 골유도성을 가진 물리적 자극으로써 골세포로의 분화, 골화 촉진 및 칼슘 유도 등 골 회복에 도움을 주는 효과를 가지고 있다. 전기 자극을 이용한 골 재생 장치가 상용화되어있지만, 대량의 골 결손에 적용되는 골 조직편 이식술에 적용하는데는 장치의 형태 및 전기 자극의 전달에서 어려움이 있다.

이에 본 논문에서는 전기 자극을 3차원 형태의 골 조직편에 집중적으로 전달할 수 있는 체내 이식형 전기 자극 장치를 설계하였고, 동물의 골 결손 모델에 적용하여 골 결손에 대한 재생정도를 평가하였다. 골 재생 장치 개발의 사전 단계로, 전기 자극을 이용하여 체내 세포배양을 할 수 있는 바이오리액터 장치를 디자인하였다. 이를 이용하여 콜라겐 스펀지에 접종된 인간 중간엽 줄기세포에 전기 자극을 인가하며 체내 배양하였다. 전기 자극을 인가하여 세포를 배양한 그룹은 전기 자극을 인가하지 않고 배양한 그룹에 비해 줄기세포 수가 23% 만큼 더 증가했으며, 줄기세포가 콜라겐 스펀지에 보다 잘 점착되는 등의 세포 건강도 향상의 결과를 얻었다.

바이오리액터 장치를 응용하여 골 결손이 발생한 부위에 줄기 세포편과 전기 자극 전극을 이식하여 줄기세포를 골 조직으로 유도하는 방식의 골 재생 방법을 통해 토끼 하악골 결손에 대한 골 재생 실험을 수행하였다. 동물의 골 결손 형태에 맞도록 폴리이미드 전극을 제작하였고, 전기 자극 장치는 실리콘으로 밀봉하였다. 전기 자극을 한 그룹이 그렇지 않은 그룹에 비해 신생골 부피가 260% 만큼 더욱 재생되는 결과를 비롯하여

전기 자극을 인가한 그룹이 다양한 골 재생 수치에서 더 우수한 신생골 형성 결과를 얻었다.

이후 골융화성이 뛰어나고 밀봉성이 우수한 액정 크리스탈 폴리머(LCP)를 장치의 기반물질로 사용하고, 무선 전력 전송 장치와 전기 자극 생성 장치를 내장한 LCP 기반의 골 재생 장치를 제작하였다. 이 장치는 골 조직편을 지지해주는 골 지지체의 역할과 전기 자극 장치의 역할을 동시에 수행할 수 있다.

이상의 결과들은 골 결손에 직접 전기 자극을 인가할 수 있는 체내 이식형 골 재생 장치를 이용한 골 재생 시술이, 골 결손의 회복을 위한 효과적이고 새로운 방법이 될 수 있음을 보여주며, 나아가 LCP를 이용한 이식형 골 재생 장치의 개발 및 체내 세포 배양과 전기 자극이 결합된 조직편 이식 시술의 개발 및 응용을 기대할 수 있다.

주요어 : 전기 자극. 이식형 장치. 골 재생. 줄기세포. LCP

학 번 : 2009-30184